Minerals Engineering 98 (2016) 328-338

Pilot scale microwave sorting of porphyry copper ores: Part 2 – Pilot plant trials

A.R. Batchelor *, R.S. Ferrari-John, C. Dodds, S.W. Kingman

Faculty of Engineering, The University of Nottingham, University Park, Nottingham, NG7 2RD, United Kingdom

* Corresponding author. Tel.: +44 (0)115 951 4080; fax: +44 (0)115 951 4115. E-mail address: andrew.batchelor@nottingham.ac.uk (A.R. Batchelor)

Keywords

Microwave; Ore; Copper; Sorting; Infrared; Pilot Scale.

Highlights

- Pilot scale microwave infrared thermal (MW-IRT) sorting of porphyry copper ores is investigated
- Pilot plant operating windows were defined from laboratory MW-IRT testing
- A larger sample size improves laboratory predicted copper recovery in the pilot plant
- ~42-50% of pilot plant tests are predicted to within ±5% copper recovery and ~85-90% to within ±10%

Abstract

An experimental pilot plant was constructed, commissioned and operated at a major porphyry copper mine to understand the challenges of microwave infrared thermal (MW-IRT) sorting at scale and to compare batch laboratory performance with pilot-scale continuous sortability performance. A method was developed to define the 95% confidence intervals on pilot plant operating windows from experiments on 50 to 150 fragments performed in a laboratory based replica of the pilot scale microwave treatment system. It appeared that the laboratory testing methodology predicted the sortability of the ores fairly well. For the 11 ore types and three size classes (-76.2+50.8mm, -50.8+25.4mm and -25.4+12.7mm) tested over 233 pilot plant experiments, approximately 42% of the better optimised pilot plant runs predicted copper recovery to within ±5% copper recovery and approximately 84% of the runs to within ±10%. These figures were improved to approximately 50% predicted to within ±5% and approximately 90% to within ±10% if the -25.4+12.7mm size class was omitted. It was demonstrated that laboratory testing better predicted pilot plant sorting performance and provided a narrower operating window when a larger sample size (>50 fragments) was considered due to improved representivity. It is, therefore, fully expected that better predictions would result from larger laboratory sample sizes than those tested during any future testing campaigns. To date, approximately 15,500 tonnes of ore has been processed through the pilot-scale test facility, generating significant engineering know-how and demonstrating MW-IRT sorting at a scale in the order of that required by the mining industry.

http://dx.doi.org/10.1016/j.mineng.2016.07.009

1 Introduction

Recent advances in automated sorting technology have seen ore sorting become an increasingly attractive possibility for the mining industry to help reduce energy consumption while maintaining productivity in the forecasted low-grade future. However, sensors that have the resolution to discern grade differences in low-grade ores (typically down to ~0.1wt%) or have the capacity to process the several thousand tonnes per hour required by the largest operating mines in an economical manner, particularly on a fragment-by-fragment basis, continue to be a limiting factor (Daniel and Lewis-Gray, 2011; Drinkwater et al., 2012; Lessard et al., 2014; Lessard et al., 2016; Napier-Munn, 2015; Pokrajcic et al., 2009; Powell and Bye, 2009). Microwave treatment followed by infrared thermal imaging (MW-IRT) has been proposed as an excitation-discrimination technique to facilitate sorting of low-grade ore (Berglund and Forssberg, 1980; Ghosh et al., 2013; Ghosh et al., 2014; John et al., 2015; Sivamohan and Forssberg, 1991; Van Weert and Kondos, 2007; Van Weert et al., 2009), but until recently has not been demonstrated at scale.

In the first part of this paper, a bespoke, laboratory-based, high throughput and continuous pilot scale microwave treatment system capable of treating up to 100t/h (instantaneous) of ore in a batch wise fashion was described (Batchelor et al., 2016; Katrib et al., 2016). Utilizing the bespoke system, the fragment-by-fragment thermal response of a variety of porphyry copper ores from different operating conditions was investigated with the aim of determining the effect on sortability performance across conditions likely to be encountered in an industrial environment. It was found that microwave treatment energy was the driving force behind the ultimate temperature rise fragments experienced and that the presence of microwave-heating gangue minerals was the main source of deviation from intrinsic, or ideal, sortability performance.

Subsequent to initial laboratory testing, a decision was taken to commission a pilot-scale test facility at a major porphyry copper mine owned and operated by the project sponsor. The aim of the facility was to understand and develop know-how surrounding the engineering challenges of microwave sorting at scale, to compare batch laboratory sortability performance with pilot-scale continuous sorting performance to validate the testing methodology and support project valuation. The pilot plant microwave treatment system had the exact same specification as the laboratory system, apart from utilizing a slightly different microwave frequency (915MHz) due to the plant being located in a region that uses a different industrial, scientific and medical (ISM) band to the UK (896MHz) (Meredith, 1998). The major difference was the extensive feed storage and preparation facilities, integration of a commercially available automated sorter, and the associated materials handling, process control, sampling, sample preparation and other facilities that would enable continuous processing for several hours of operation covering a typical working shift. Pilot plant testing was conducted over a period of one and a half years, during which time approximately 300 test runs were completed on 11 different ore types with a total of approximately 15,500 tonnes of material processed.

This second part of the paper presents a comparison of the laboratory and pilot plant sortability performance and further develops the testing methodology to give confidence in the prediction of pilot sortability performance from laboratory testing.

2 Materials and methods

2.1 Ore samples

The porphyry copper ore samples used throughout the piloting investigation were all sourced from the pilot plant host mine. 11 ore types were selected that covered a range of different lithologies with varying copper sulphide grade, copper sulphide to iron sulphide ratio and non-sulphide gangue mineralogy. The ores were also selected on the basis of proportion of future mine plan or otherwise potentially economically valuable material. The ores were supplied in three narrow size classes, namely -76.2+50.8mm, -50.8+25.4mm and -25.4+12.7mm, listed in Table 1, for the reasons outlined in the first part of this paper (Batchelor et al., 2016). Each size class was tested separately to enable optimal separation efficiency from the sorter.

The mine selected an ore-grade and waste-grade (denoted with the suffix “W”) version of four lithologies plus a waste-grade version of three lithologies. Samples #9 and #9W were a quartz-monzonite ore diluted with approximately 10-20wt% quartzite fragments, which had a consistent texture of well disseminated microwave-heating phases within a speccled microwave-transparent. Samples #10 and #10W were a quartzite ore, which had a fairly consistent texture of well disseminated microwave-heating phases within the microwave-transparent matrix, with some coarser and clustered mineralisation and some sulphide veins. Samples #11 and #11W were a limestone-skarn ore, which had a wide variety of textures from well disseminated to very coarse and clustered microwave-heating phases within the microwave-transparent matrix. The aforementioned samples were previously reported in the first part of this paper (Batchelor et al., 2016). Additional samples, namely #14, #14W, #15W, #16W and #17W were all varieties of monzonite ore with similar textural characteristics to samples #9 and #9W without the quartzite dilution.

http://dx.doi.org/10.1016/j.mineng.2016.07.009

Table 1

Sample list and number of fragments tested/analysed in the laboratory

Sample ID	Sample Grade *	-76.2+50.8mm	-50.8+25.4mm	-25.4+12.7mm
9	Ore	100/50	100/50	150/150
9W	Waste	50/50	50/50	50/50
10	Ore	100/100	100/100	100/100
10W	Waste	100/50	100/50	100/50
11	Ore	100/50	100/50	100/50
11W	Waste	140/140	150/150	150/150
14	Ore	150/150	150/150	150/150
14W	Waste	140/140	150/150	150/150
15W	Waste	150/150	150/150	150/150
16W	Waste	150/150	150/150	150/150
17W	Waste	150/150	150/150	150/150

* Sample defined as “ore-grade” or “waste-grade” by host mine.

Indicative modal mineralogies for the -50.8+25.4mm size samples were estimated by using a Mineral Liberation Analyser (MLA) (FEI, 2016) to measure polished sections of 20 representatively split lump fragments, reported in the first part of this paper. Samples #14, #14W, #15W, #16W and #17W were not analysed using the MLA. The dominant copper sulphide mineral in all samples was chalcopyrite. The dominant sulphide gangue was pyrite and other microwave-heating gangue included montmorillonite and iron oxides. The dominant non-sulphide and microwave-transparent gangue minerals were quartz, feldspar and mica. The limestone-skarn ores also had significant proportions of pyroxenes, amphiboles, garnets and carbonates.

Any fragments that contained <0.1%Cu were considered to be effectively barren and uneconomic to process according to the project sponsors, and were then necessarily the main target for rejection. Processing economics further dictated that fragments between 0.1 and 0.25%Cu were of marginal grade or mineralised waste. The higher grade fragments were arbitrarily divided into 0.25–0.5%Cu, 0.5–1%Cu and >1%Cu by the authors to see the mass and copper distributions across different fragment grade classes, given in Table S.1 in the Supplementary Information.

2.2 Pilot scale microwave sorting facility

The pilot plant was used as a treatment and sorting test facility and was not integrated with any downstream processing. The pilot plant is located on the host mine site adjacent to the mill, shown in Figure 1. Run-of-mine (ROM) ore is diverted from the primary crusher and taken by truck to a mobile crushing and screening facility where it is prepared into the three size classes. The sized ore is then taken by truck to the pilot plant stockpile. Ore is transferred to the feed loading bay by a loader where it is first passed through a sampling station before being conveyed into the main building. Upon entering the building the ore is washed and partially blow dried with compressed air over a vibrating screen to remove dust and chips before being stored in an insulated feed conditioning bin to equilibrate the fragment temperature.

The subsequent microwave treatment and sorting process is illustrated in Figure 2. The ore is fed by a belt feeder, over a vibrating screen to remove any remaining chips, to the microwave treatment belt at a pre-determined throughput and immediately imaged under an infrared thermal camera to capture the feed temperature distribution. The material passes through the microwave cavity at a pre-determined power level and belt speed to receive the required treatment energy. Upon exiting the cavity, the material passes over an intermediary belt to accelerate the fragments before moving on to the sorter belt moving at a higher speed to allow the fragments to spread out to the required spacing for interrogation by the post-microwave treatment infrared thermal camera and laser scanner for fragment tracking. The fragment thermal equilibration time was in the order of 10 to 30 seconds depending on the microwave treatment belt speed employed. In the current arrangement, only the top-facing fragment surface was interrogated by the thermal camera. The pre-determined sorting decision is implemented and the pneumatic actuators blast the lowest mass fraction (either accepts or rejects, although for the purposes of illustration rejects (or Colds) have been used) to save energy and minimise work rate. The two product streams are conveyed though product sampling stations to retention bays from where they may be collected for re-use or transfered to the ROM stockpile at the mill.

http://dx.doi.org/10.1016/j.mineng.2016.07.009

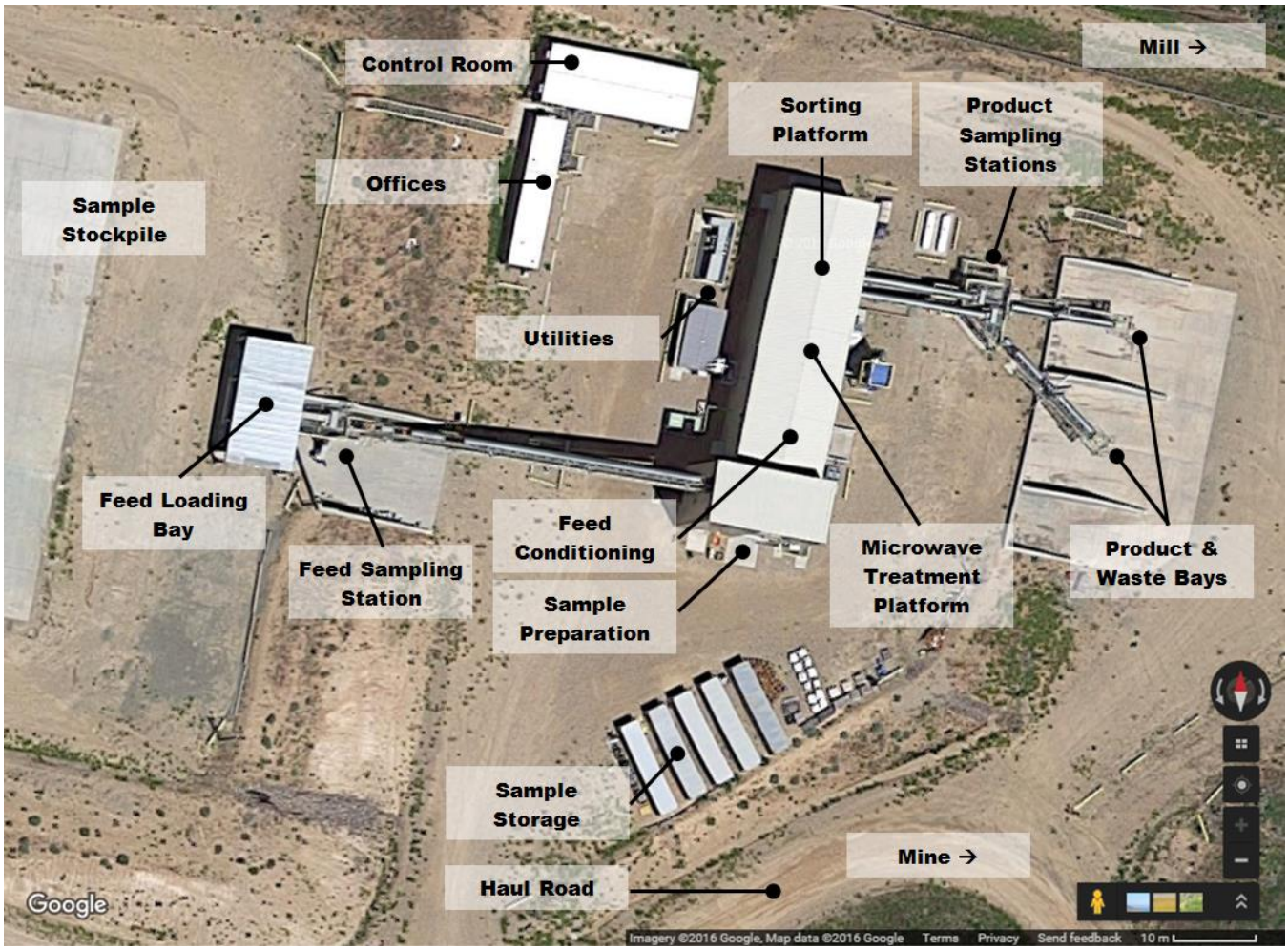

Figure 1: Pilot plant aerial view

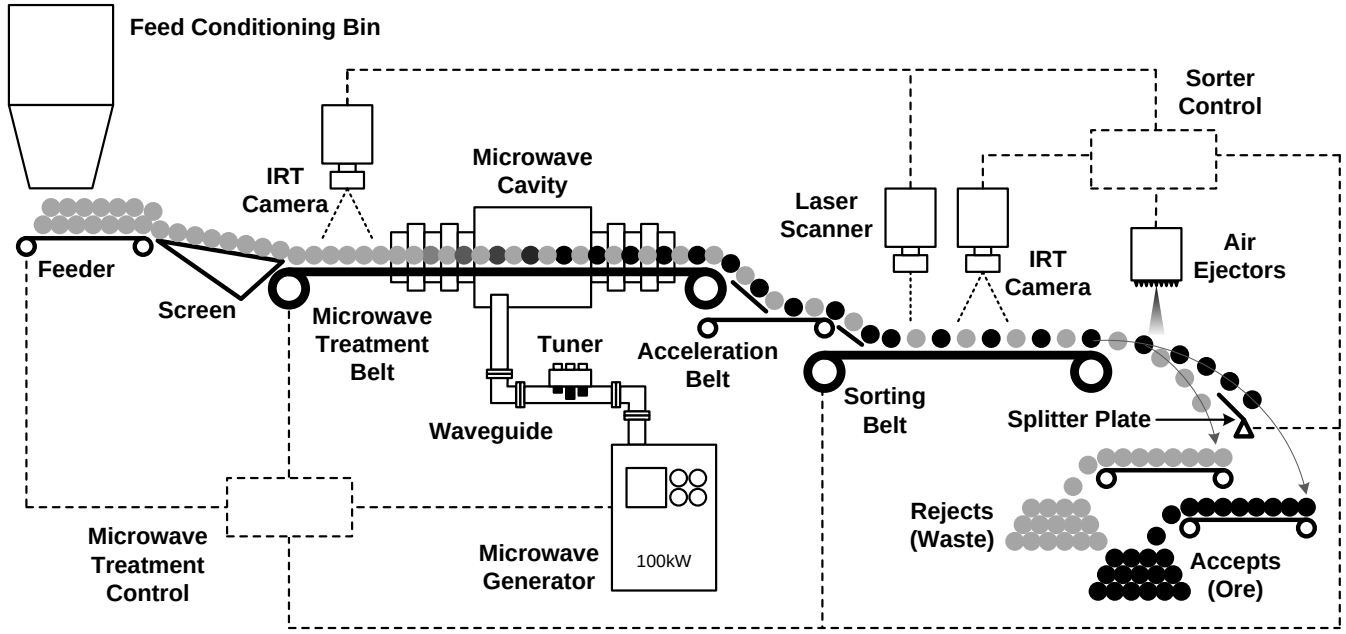

Figure 2: Microwave treatment and sorting system

http://dx.doi.org/10.1016/j.mineng.2016.07.009

2.3 Testing methodology

Approximately 200kg of ore was received at the laboratory and a test sample was representatively split, washed, dried, labelled and weighed. A variety of process conditions were tested according to the methodology described in the first part of this paper (Batchelor et al., 2016), which typically comprised testing of two to three doses at one or two belt speeds, with two fragment orientations and one or two fragment positions within the cavity. An NEC H2640 infrared thermal camera was used to capture the thermal images and Radiometric Complete software used to extract the temperature information. The sortability curves were interrogated and a set of test conditions recommended to the pilot plant operators with the aim of maximising throughput while providing a suitable temperature rise to make as clean a separation as possible without over-heating the hottest fragments (<80°C). Recommended microwave treatment doses were typically in the range of 0.5–1kWh/t.

In the pilot plant, the feeder and microwave belt speed was configured to achieve the required throughput to provide a monolayer of the ore with an initial microwave power input of 10kW applied. Power was subsequently increased up to the recommended setting. Power input and throughput (i.e. feed rate and belt speed) could then be increased linearly to maintain dose and the fragment monolayer presentation while maximising throughput. For the case of the -25.4+12.7mm size fraction in particular, a multilayer could potentially be used to increase throughput as well without overloading the belt. Alternately, if the target power input did not allow for stable treatment (due to intermittent arcing, which is a probabilistic effect of fragment shape, surface mineralisation and electric field distribution within the cavity) then belt speed and throughput could be reduced linearly to maintain dose at the maximum achievable power input. It is worth noting that the pilot plant ore was treated damp (typically <1% free surface moisture) as opposed to an air dried basis in the laboratory, as this was required to prevent dust accumulation within the microwave cavity as well as assisting to equilibrate the feed temperature.

2.4 Thermal analysis methodology

In the laboratory, the recommended temperature cut-point was determined based on the average fragment temperature rise (ΔT_{ave}); that is, the average fragment temperature post-microwave treatment minus the average fragment temperature pre-microwave treatment. The pilot plant uses a different analysis to determine whether a fragment is to be considered hot or cold and, therefore, a target for rejection. The thermal analysis determines if a fragment has a certain, user defined percentage of the surface area (typically 40-60%) above or below a user defined threshold temperature rise value (ΔT_{cut}) based on the initial average feed temperature.

In essence, this method identifies a heat bloom on the surface of the fragments that is indicative of the presence of microwave-heating minerals within the fragment. Given the software available in the laboratory, it was very laborious to try to replicate this decision making process and so it was not performed as a matter of routine. Nevertheless, the raw data was available and a limited number of analyses were conducted to compare the fragments selected by the two methods and it was found that the vast majority of the same fragments were selected by both methods over a wide range of surface area and temperature threshold values, particularly for the hotter fragments, as illustrated in Figure 3 and Table 2 for the sample #9 -50.8+25.4mm size class.

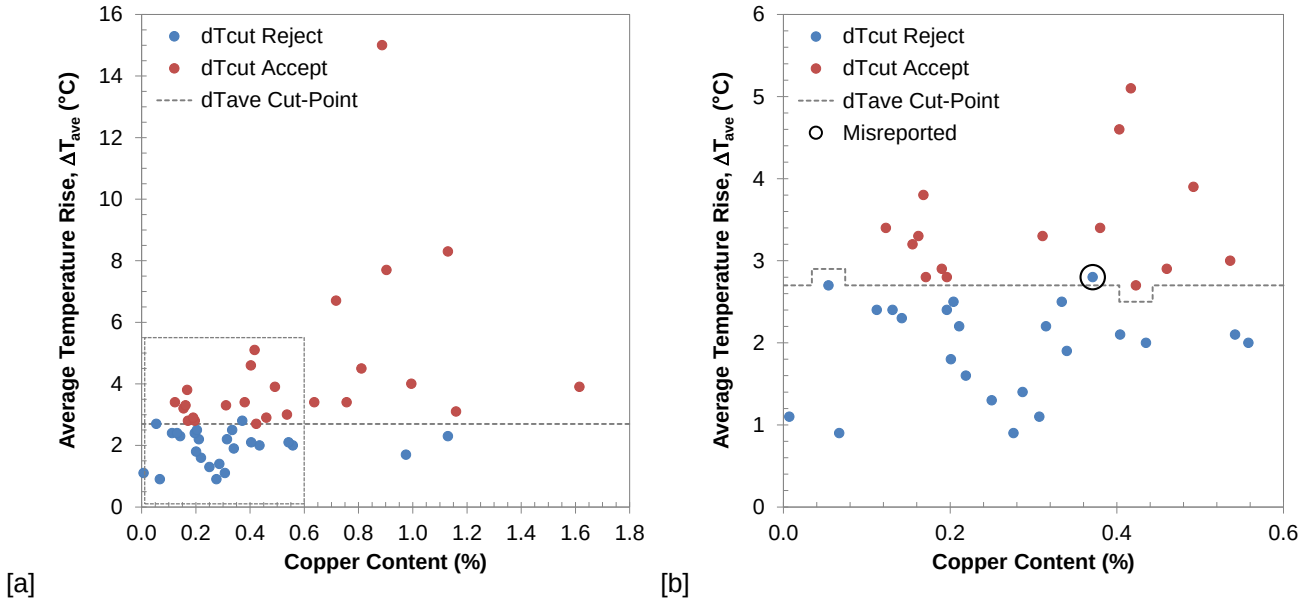

Figure 3: Sorting decision fragment selection comparison example (sample #9, -50.8+25.4mm)

http://dx.doi.org/10.1016/j.mineng.2016.07.009

Table 2 shows the range of ΔT_{cut} values that would be required to achieve a sort that accepts 25%, 50% and 75% of the hot fragments by mass for a given area percentage using the pilot plant method with laboratory data. It can be seen that the mass and copper recoveries obtained from the fragments selected by this method are quite close considering only 50 fragments were interrogated. Figure 3 plots the laboratory method, using a ΔT_{ave} cut-point of 2.7°C to achieve a 50% mass recovery to accepts, versus the pilot plant method requiring 40% of the fragment surface area to be greater than a ΔT_{cut} cut-point of 2.85°C. In the example given, only one fragment out of 50 misreports from the accepts stream to the rejects stream according to the pilot plant method, with two fragments potentially going either way according to the laboratory method as they both have an average temperature rise equal to the ΔT_{ave} cut-point.

Table 2

Sorting decision according to different fragment areas and cut point thresholds

Accept 25% Hots, Blast Hots						Accept 50% Hots, Blast Hots/Colds						Accept 75% Hots, Blast Colds					
Area % Above ΔT_{cut} (°C)	Area % Below ΔT_{cut} (°C)	Cut Point ΔT_{cut} (°C)	Mass Recovery %	Cu Recovery %	Cu Grade %	Area % Above ΔT_{cut} (°C)	Area % Below ΔT_{cut} (°C)	Cut Point ΔT_{cut} (°C)	Mass Recovery %	Cu Recovery %	Cu Grade %	Area % Above ΔT_{cut} (°C)	Area % Below ΔT_{cut} (°C)	Cut Point ΔT_{cut} (°C)	Mass Recovery %	Cu Recovery %	Cu Grade %
10	90	4.35-4.45	25.2	40.8	0.673	10	90	3.35	50.2	60.9	0.503	10	90	2.6	73.1	81.1	0.460
15	85	4.2	25.8	43.2	0.696	15	85	3.25	50.2	60.9	0.503	15	85	2.4	76.7	82.8	0.449
20	80	4.15	24.3	40.5	0.693	20	80	3.15	50.2	60.9	0.503	20	80	2.35	76.7	82.8	0.449
25	75	4-4.05	24.3	40.5	0.693	25	75	3.05	51.4	61.4	0.495	25	75	2.3	76.7	82.8	0.449
30	70	3.85-3.9	24.3	40.5	0.693	30	70	3	47.9	60.9	0.528	30	70	2.2-2.25	76.7	82.8	0.449
35	65	3.5-3.65	25.8	43.2	0.696	35	65	2.9	51.2	64.3	0.521	35	65	2.15-2.2	76.7	82.8	0.449
40	60	3.4-3.45	25.8	43.2	0.696	40	60	2.85	49.7	63.0	0.526	40	60	2.1-2.15	76.7	82.8	0.449
45	55	3.25-3.3	25.6	42.3	0.685	45	55	2.7-2.8	49.7	63.0	0.526	45	55	2.15	74.9	80.6	0.446
50	50	3.2	25.6	42.3	0.685	50	50	2.6-2.7	49.7	63.0	0.526	50	50	2.05-2.1	74.9	80.6	0.446
						ΔT_{ave}		2.7	51.2	64.3	0.521						

The fragment surface area and temperature rise settings were initially estimated by the pilot plant operators and then adjusted to achieve the target mass rejection for the given run, as determined based on average temperature rise cut-point from laboratory testing. As mentioned previously, the product with the lowest mass fraction (either hot or cold fragments) was chosen to be blasted. Once steady state had been reached at the desired conditions the two products were sampled over the duration of the run, then representatively sub-sampled and submitted for assay to enable calculation of sortability performance.

2.5 Data analysis methodology

The laboratory recommended settings took the form of a sortability curve (cumulative mass and copper recovery curve, or yield-recovery curve) for the most stable fragment orientation (i.e. resting on their flattest surface simulating the most probable resting orientation obtained in the pilot plant, O1) in one position in the cavity, with associated tabulated separation data at given temperature cut-points or mass rejections. However, it is evident that in the pilot plant any given fragment may fall in one of many orientations under the thermal camera or positions in the cavity during treatment. In order to account for the random nature of particle presentation, an operating window was determined based on the potential temperature rise variation from orientation and cavity position measured in the laboratory.

Analysis of all of the positional data yielded average temperature rise relative standard deviations (%rsd) of approximately 30%, 15% and 20% for the -76.2+50.8mm, -50.8+25.4mm and -25.4+12.7mm size classes respectively. It was shown in the first part of this paper that fragment position in the cavity had only a small effect on sortability performance, since the hottest fragments always remain hot compared to the lower grade cold fragments. A bootstrap analysis was conducted with 1,000 replicates where the individual fragment average temperature rise values were randomly varied according to one of two orientations and then augmented by a normally distributed variation due to position in the cavity. The 95% confidence limits for the sortability curves could then be determined to show the window within which the sortability curves would be most likely to occur. The total fragment surface area (average of the two orientations measured, O_{ave}) average temperature rise was then used as the basis for calculating the expected average sortability performance.

http://dx.doi.org/10.1016/j.mineng.2016.07.009

3 Pilot plant commissioning

Following construction of the pilot plant several commissioning activities were undertaken to improve the operation of the plant. It is not within the remit of this paper to describe them all; however, there were two important aspects that directly relate to the comparison of sortability performance that require attention, namely optimisation of sorter blast efficiency and characterisation of the feed temperature distribution prior to microwave treatment.

3.1 Sorter blast efficiency

Sorter blast efficiency is the percentage of target particles that are correctly blasted and gives a measure of the percentage of particles that misreport to a product stream. Correct ejection is influenced by factors such as particle size and shape, trajectory off the sorting belt, spacing and clustering on the sorting belt, and the air ejection pressure and pattern. The sorter setup was thus dependent on the ore type (e.g. angular quartzite versus rounded pebbles) and feed size (i.e. -76.2+50.8mm, -50.8+25.4mm or -25.4+12.7mm), which is why the size classes were treated separately. Prior to optimisation in early plant runs the sorter blast efficiency was approximately 85%; that is, approximately 15% of the fragments misreported to the incorrect product stream. After extensive testing the efficiency was increased up to approximately 95% for the -76.2+50.8mm and -50.8+25.4mm size classes (Harding, 2013). Following the optimisation work, the -25.4+12.7mm sizes reportedly suffered from some fragment clustering on the sorter belt for some ores, which prevented the sorter efficiency from reaching 95%.

3.2 Feed temperature distribution variation

In the laboratory, the pre-microwave treatment temperature was measured for each individual fragment to enable an accurate measurement of average temperature rise for every fragment post-microwave treatment. However, in the pilot plant it was not possible to measure the pre-treatment temperature for each individual fragment due to the inability to delineate fragment boundaries on closely packed particles with very similar temperatures at high throughputs. This introduced an amount of uncertainty in the average temperature rise that was proportional to the amount of variation in the feed temperature distribution, thereby adversely affecting the sorting decision particularly for discrimination of the colder fragments. There were two feasible ways to combat this problem: increase the microwave treatment energy to ensure that the temperature rise of the coldest fragments is in excess of the feed temperature variation, or minimise the feed temperature variation to an acceptable level. Increasing the treatment energy comes with a higher operating cost and potentially limits throughput for a fixed installed power. It was therefore decided to find a means of reducing the feed temperature variation.

Temperature variation was described by a range of four standard deviations (4σ); that is, $\pm 2\sigma$ around the mean, giving approximately 95% confidence intervals on the pre-treatment temperature. It was estimated that $4\sigma < 1$°C would be required to achieve acceptable sorting performance at the treatment energies commonly employed and this condition was typically met during laboratory testing. Surveys were conducted of the mine site to measure the temperature and 4σ variation at various stages in the flow sheet, shown in Figure 4. The 4σ variation observed in the pilot plant was also surveyed prior to the implementation of measures to reduce feed temperature variation. It can be seen that depending on the prevailing conditions at the time of the surveys the microwave feed temperature variation could be up to $4\sigma > 3$°C, which was estimated to introduce a sorting error of approximately 30-50%. After implementation of measures to reduce feed temperature variation (which cannot be detailed at this time for confidentiality reasons) the variation was consistently $4\sigma < 1$°C, which was estimated to introduce a sorting error of less than 5% (Harding, 2013).

http://dx.doi.org/10.1016/j.mineng.2016.07.009

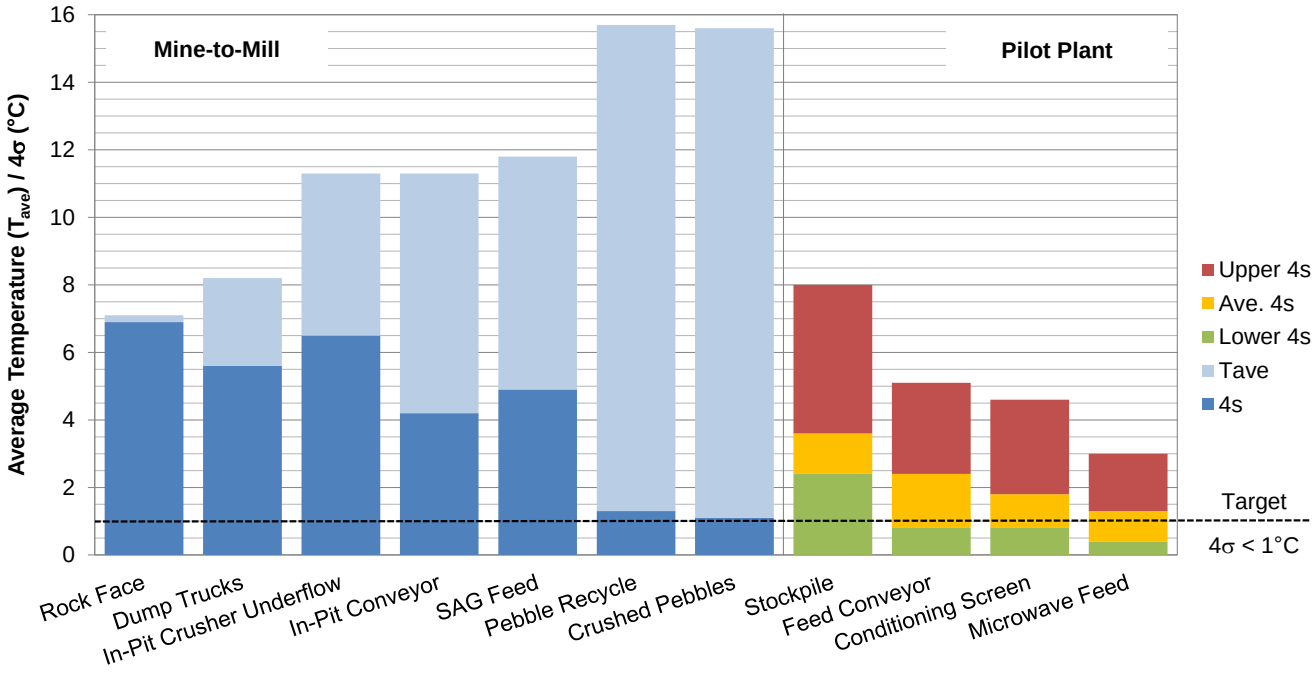

Figure 4: Ore temperature variation across mine site

4 Ore sortability performance

4.1 Analysis of individual samples

The pilot plant typically ran a series of setup tests for a period of approximately 30 minutes each to determine how the ore responded to treatment at the recommended settings. Longer tests of typically six hours were then run to assess system performance across a shift with changes made to the test conditions as necessary. For some ores, a series of exploratory tests were performed for a period of approximately 30 to 60 minutes each to evaluate the effect of varying test conditions and temperature cut-point decision making.

Figure 5, Figure 6 and Figure 7 give the intrinsic, laboratory, and pilot plant sortability curves for samples #9, #10 and #11W respectively. The three samples illustrate sortability performance for the three main ore types, different sample sizes and three types of pilot plant run tested. The sortability curves for the additional samples are given in Figure S.1 to Figure S.8 in the Supplementary Information and demonstrate similar trends. The plots also show the 95% confidence windows of the sortability curves for variation according to fragment orientation (0%rsd), and both fragment orientation and fragment position in the cavity (30%rsd, 15%rsd or 20%rsd for -76.2+50.8mm, -50.8+25.4mm or -25.4+12.7mm respectively). The pilot plant setup, run and exploratory tests are also superimposed to illustrate how close each test came to the laboratory predicted sortability curve.

It is evident that many of the pilot plant tests fall within the window defined by variation in orientation and most within the window defined by variation in orientation and position in the cavity for the -76.2+50.8mm and -50.8+25.4mm size fragments. This was particularly true for ores where 100 to 150 fragments were tested in the laboratory, as the larger sample set provided a better estimation of the sortability performance through greater sample representivity. The exploratory tests demonstrated that a range of copper recovery values were obtained at a similar mass recovery to accepts depending on the test and thermal decision conditions chosen. Therefore, it is possible that more extensive optimisation of these conditions may have resulted in a closer match to laboratory predicted sortability curves.

Most of the variability from the average total fragment surface temperature sortability (O_{ave}) was accounted for by fragment orientation. This was particularly true for the coarser fragments where the difference in average temperature rise was significantly different from one side of a fragment to the other. The 15-30% normally distributed variation in fragment orientation temperature attributed to position in the cavity typically only marginally extended the range of the operating window. This result was as expected due to position in the cavity not contributing to a significant reordering of the fragments on an average temperature rise basis when considered separately, as the hot fragments remained hot and the cold fragments remained cold (Batchelor et al., 2016).

The pilot plant tests on the -25.4+12.7mm size fragments frequently significantly under-performed what was expected from laboratory testing. As mentioned previously, this was largely due to issues with fragment clustering on the sorting belt, which remained unresolved throughout the piloting campaign. Nevertheless, many tests yielded results similar to that predicted in the laboratory when the sorter was running well.

http://dx.doi.org/10.1016/j.mineng.2016.07.009

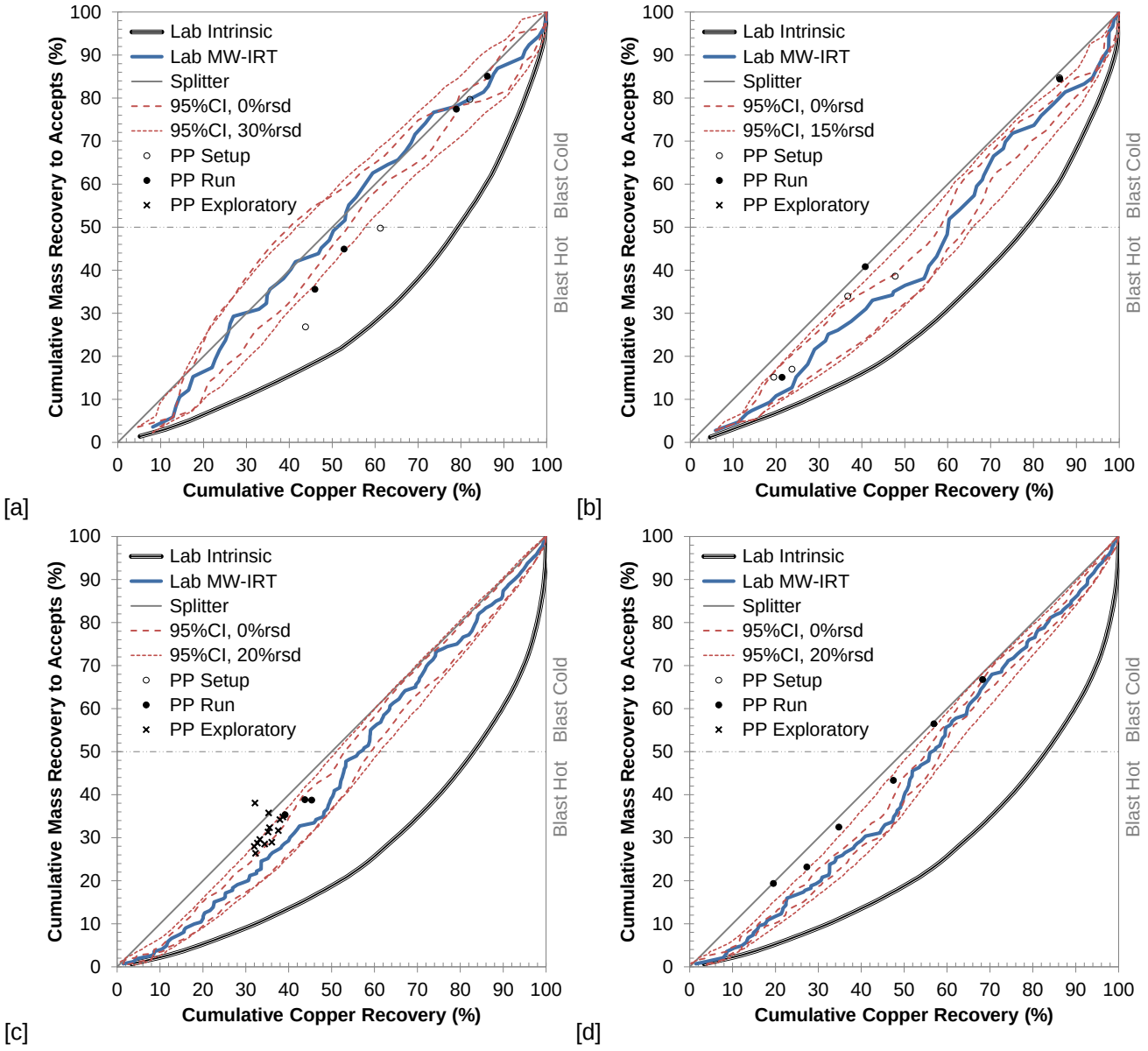

Figure 5: Sample #9 sortability performance for [a] -76.2+50.8mm fragments at ~0.75kWh/t, [b] -50.8+25.4mm fragments at ~1kWh/t, [c] -25.4+12.7mm at ~1kWh/t, and [d] -25.4+12.7mm at ~0.75kWh/t

Furthermore, it is evident that sortability curves that are defined by 100 to 150 fragments have narrower operating windows. Smaller sample sets in the laboratory (i.e 50 fragments) that contained a few fragments with a significant proportion of the copper (e.g. >5-10% of the total copper in one fragment) tended to result in large movements in the predicted copper recovery if the ordering of the fragments changed when attributing variation according to orientation and position in the cavity. By increasing the number of measured fragments, no single fragment contained such a large proportion of the copper and any reordering from colds to hots resulted in a smaller shift in copper recovery for a given mass recovery. Increasing the size of the sample set in the laboratory thus defines a narrower predicted operating window as well as improving representivity for improved sortability estimation.

A qualitative observation from the laboratory testing was that samples with a wider range in average temperature rise (e.g. ΔT_{ave} ranging from 0-20°C as opposed to 0-5°C) tended to yield a narrower operating window. It was difficult to isolate this apparent effect from other variables (such as sample size, variation due to orientation and copper distribution across fragments) but it was believed to be due to fragments having a larger thermal difference relative to each other, which limited reordering of the fragments when the bootstrap analysis was conducted. Therefore, it may be inferred that utilizing a higher microwave treatment energy to raise the fragment temperatures to a practical maximum (subject to energy costs, throughput penalty, etc.) would help to more accurately predict the expected pilot plant sortability performance.

http://dx.doi.org/10.1016/j.mineng.2016.07.009

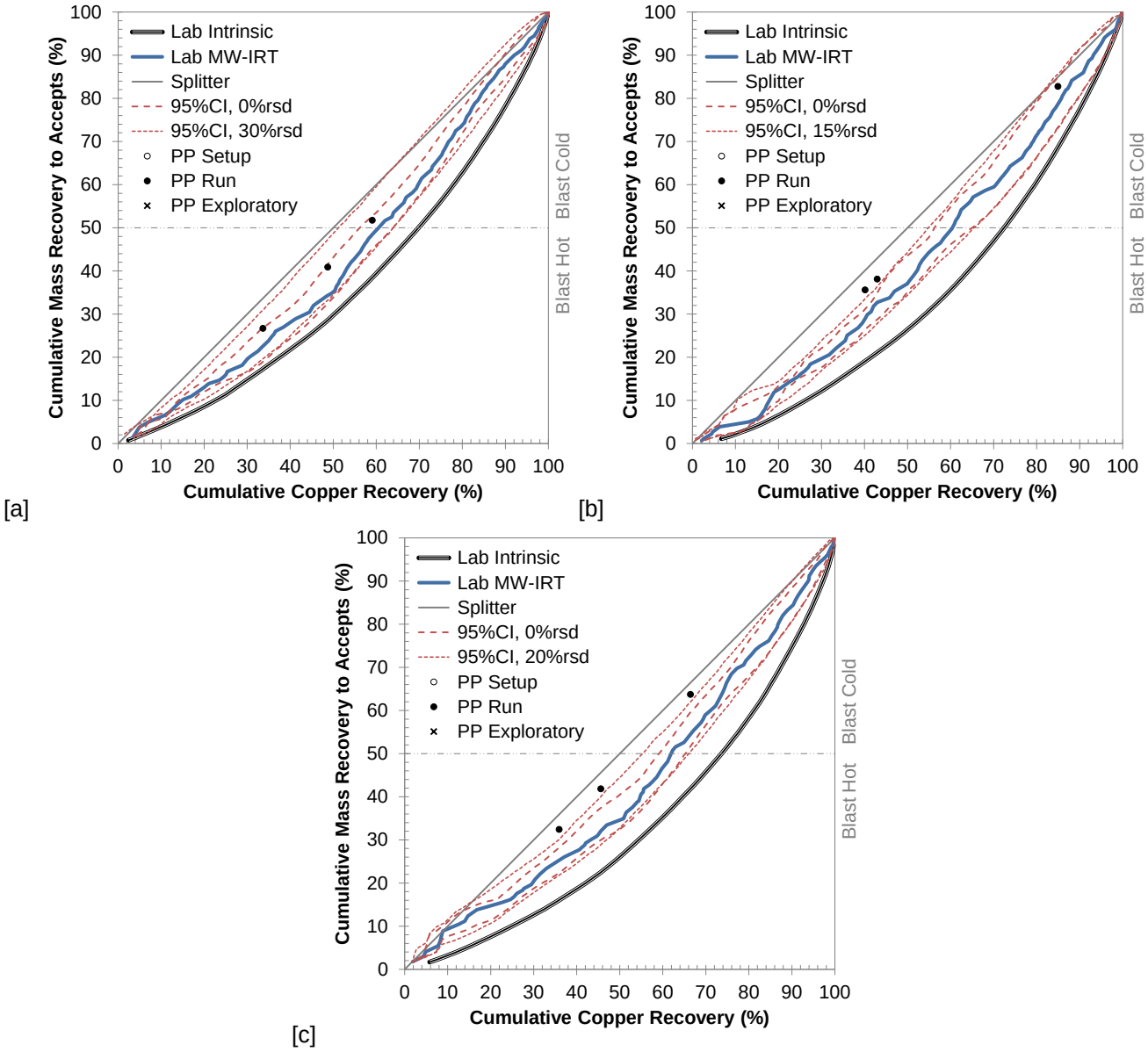

Figure 6: Sample #10 sortability performance for [a] -76.2+50.8mm fragments at ~0.75kWh/t, [b] -50.8+25.4mm fragments at ~0.75kWh/t, and [c] -25.4+12.7mm at ~1kWh/t

http://dx.doi.org/10.1016/j.mineng.2016.07.009

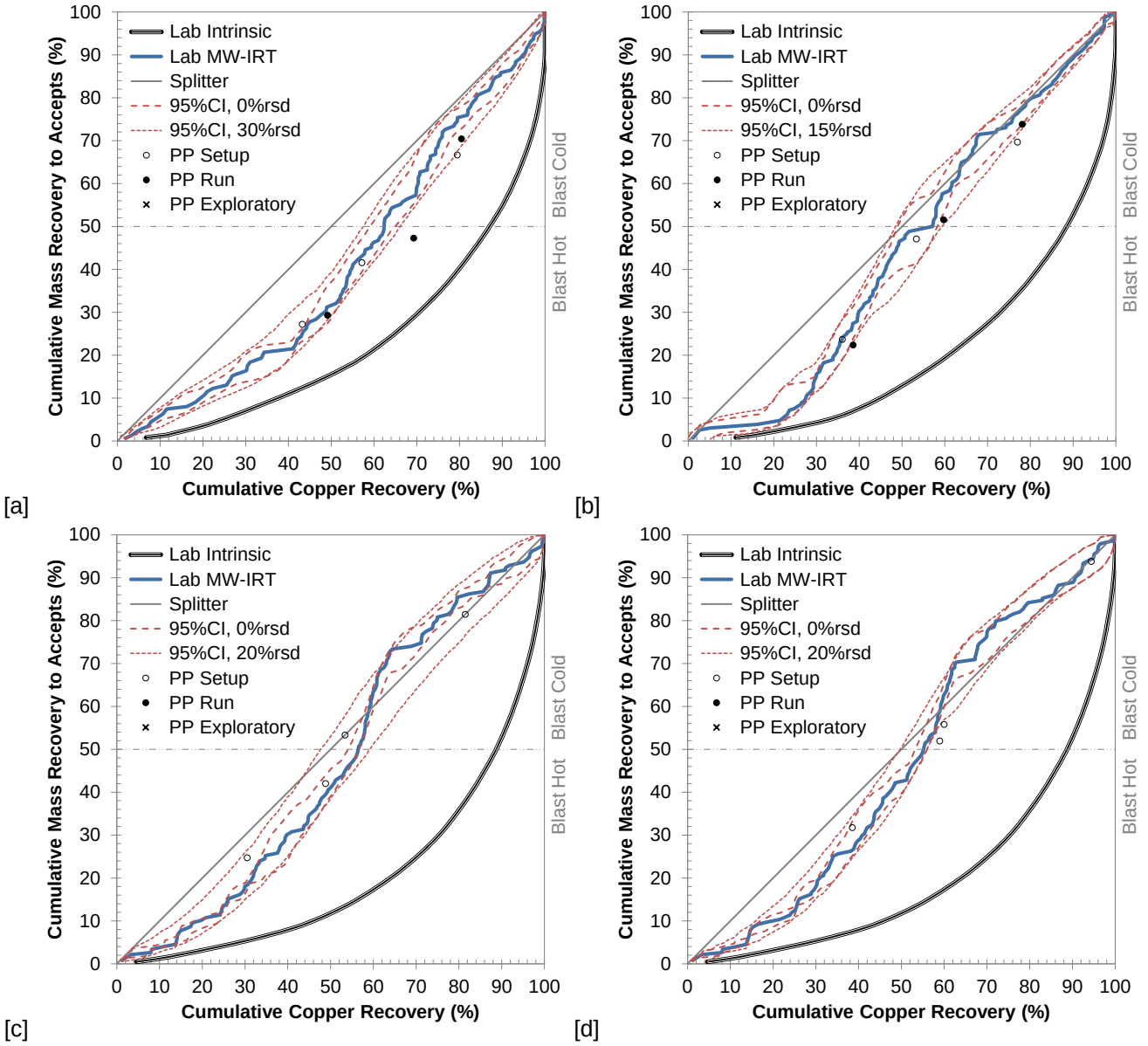

Figure 7: Sample #11W sortability performance for [a] -76.2+50.8mm fragments at ~0.75kWh/t, [b] -50.8+25.4mm fragments at ~0.75kWh/t, [c] -25.4+12.7mm at ~1kWh/t, and [d] -25.4+12.7mm at ~0.5kWh/t

http://dx.doi.org/10.1016/j.mineng.2016.07.009

4.2 Laboratory versus pilot plant separations

All of the pilot plant tests (including the additional samples #14, #14W, #15W, #16W and #17W) have been collated by size class and in total. Figure 8 gives the laboratory versus pilot plant copper recovery values at the corresponding mass recovery to accepts from the pilot plant. Figure 9 gives the difference in copper recovery values plotted as histograms. The average difference between the pilot plant runs (i.e. excluding setup and exploratory tests) and the laboratory for the -76.2+25.4mm combined size classes was -2% (i.e. the laboratory tests slightly over-predicted sorting performance on average) with a 90% confidence interval of ±9.7%. It would be expected that improving representivity of the many laboratory tests that only considered 50 fragments would reduce this confidence interval. However, for the -76.2+25.4mm material in the campaign currently under investigation approximately 50% of the pilot plant runs achieved a copper recovery prediction within ±5% and 90% of the runs within ±10%. Including the -25.4+12.7mm size class, approximately 42% of the pilot plant runs achieved a copper recovery prediction within ±5% and 84% of the runs within ±10%.

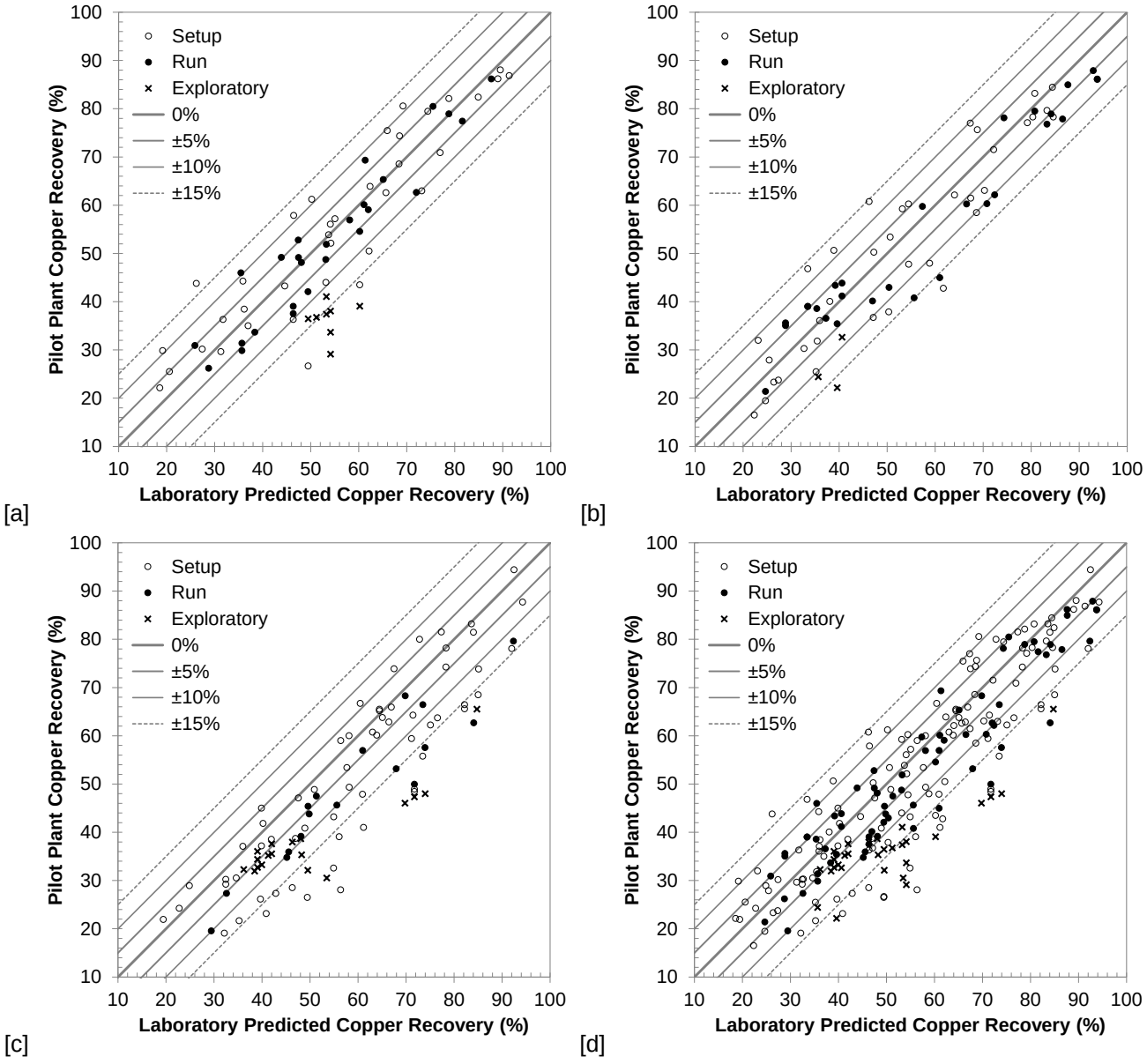

Figure 8: Laboratory predicted copper recovery versus pilot plant copper recovery for a given pilot plant mass recovery for [a] -76.2+50.8mm fragments, [b] -50.8+25.4mm fragments, [c] -25.4+12.7mm fragments, and [d] all fragments (-76.2+12.7mm)

http://dx.doi.org/10.1016/j.mineng.2016.07.009

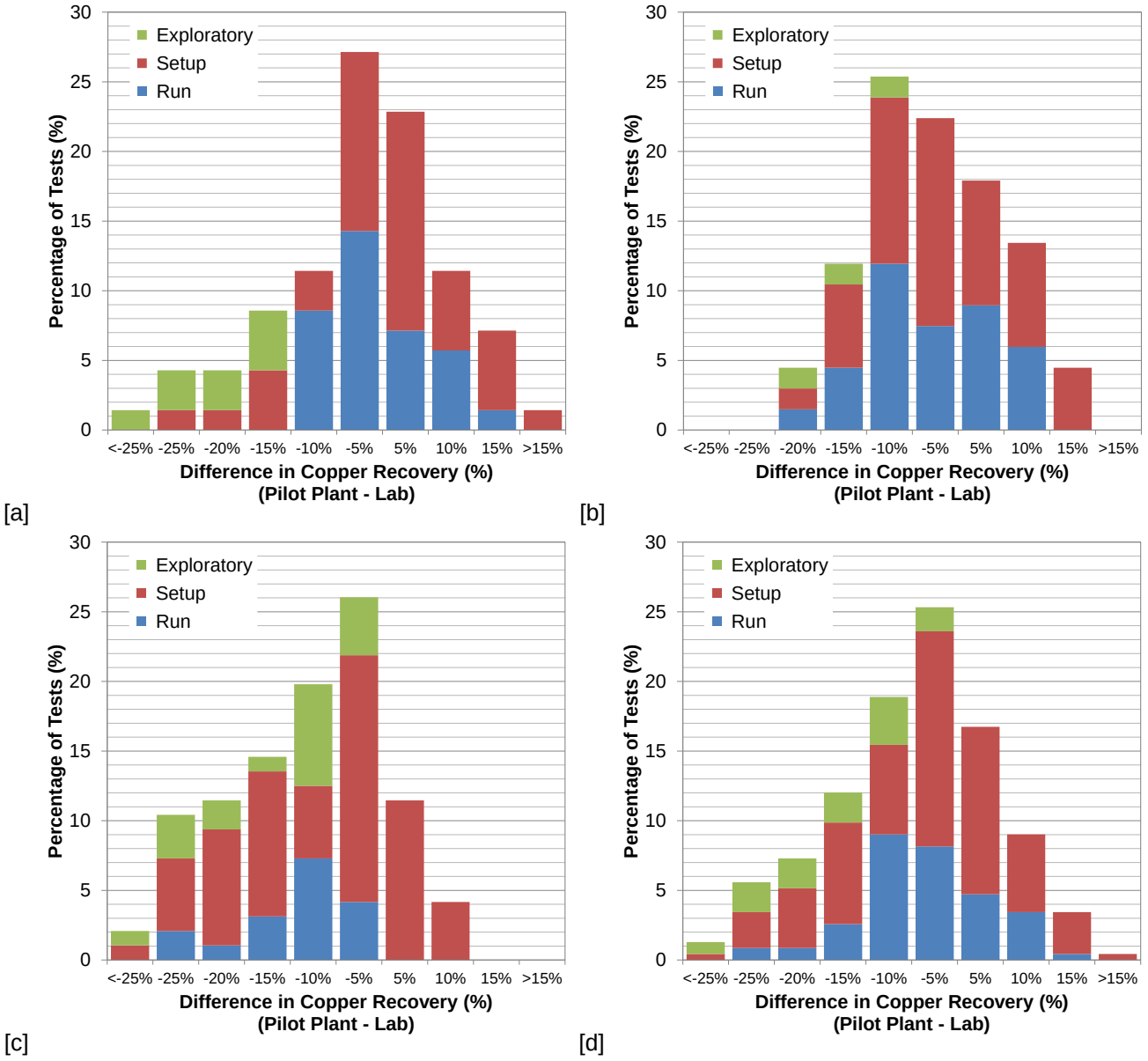

Figure 9: Difference between laboratory predicted copper recovery and pilot plant copper recovery for a given pilot plant mass recovery for [a] -76.2+50.8mm fragments, [b] -50.8+25.4mm fragments, [c] -25.4+12.7mm fragments, and [d] all fragments (-76.2+12.7mm)

http://dx.doi.org/10.1016/j.mineng.2016.07.009

5 Conclusions

A pilot scale test facility was constructed, commissioned and operated at a major porphyry copper mine to understand the challenges of MW-IRT sorting at scale and to compare batch laboratory with pilot scale continuous sortability performance.

A method was developed to define the 95% confidence intervals on pilot plant operating windows from experiments on 50 to 150 fragments performed in a laboratory based replica of the pilot scale microwave treatment system. The method incorporated average temperature rise variation due to fragment orientation as the pilot plant only imaged the surface from one side of a fragment during its sorting decision. It was demonstrated that laboratory testing better predicted pilot plant sorting performance and provided a narrower operating window when a larger sample size (>50 fragments) was considered due to improved representivity.

Given the limited number of fragments tested in the laboratory for many ore samples, a sorting error of up to approximately 10% that was introduced from both sorter blast efficiency and feed temperature variation, thermal imaging of only one side of the fragments and partial optimisation of the thermal decision conditions, it appears that the laboratory testing methodology has predicted the sortability of the ores fairly well. For the 11 ore types and three size classes (-76.2+50.8mm, -50.8+25.4mm and -25.4+12.7mm) tested over the 233 pilot plant experiments reported, approximately 42% of the better optimised pilot plant runs predicted copper recovery to within ±5% copper recovery and approximately 84% of the runs to within ±10%. These figures were improved to approximately 50% predicted to within ±5% and approximately 90% to within ±10% if the -25.4+12.7mm size class was omitted, as this size class frequently suffered from fragment clustering on the sorting belt, which remained unresolved from commissioning activities. It is fully expected that better predictions would result from larger laboratory sample sizes during any future testing campaigns.

In the first part of this paper, the fundamental basis for MW-IRT sorting along with operational and mineralogical considerations was described to demonstrate that MW-IRT sorting could provide attractive separations to reject effectively barren (<0.1wt%Cu) ore fragments. To date, approximately 15,500 tonnes of ore has been processed through the pilot scale test facility, generating significant engineering know-how and demonstrating MW-IRT sorting at a scale in the order of that required by the mining industry.

Acknowledgements

The authors greatly acknowledge Rio Tinto Technology and Innovation along with their research and industry partners for engagement and collaboration throughout the Copper NuWave™ project.

http://dx.doi.org/10.1016/j.mineng.2016.07.009

References

Batchelor, A.R., Ferrari-John, R.S., Katrib, J., Udoudo, O.B., Jones, D.A., Dodds, C., Kingman, S.W., 2016. Pilot scale microwave sorting of porphyry copper ores: Part 1 - Laboratory investigations. Minerals Engineering 98, 308-327.

Berglund, G., Forssberg, E., 1980. Seletiv uppvarmning med mikrovagor, Minfo Rapport, 0703, Sweden.

Daniel, M., Lewis-Gray, E., 2011. Comminution efficiency attracts attention. The AusIMM Bulletin 5, 18-28.

Drinkwater, D., Napier-Munn, T.J., Ballantyne, G., 2012. Energy reduction through eco-efficient comminution strategies, 26th International Mineral Processing Congress, IMPC 2012: Innovative Processing for Sustainable Growth-Conference Proceedings. Technowrites, pp. 1223-1229.

FEI, 2016. Mineral Liberation Analyser (MLA), http://www.fei.com/products/sem/mla/.

Ghosh, A., Nayak, B., Das, T.K., Palit Sagar, S., 2013. A non-invasive technique for sorting of alumina-rich iron ores. Minerals Engineering 45, 55-58.

Ghosh, A., Sharma, A.K., Nayak, B., Sagar, S.P., 2014. Infrared thermography: An approach for iron ore gradation. Minerals Engineering 62, 85-90.

Harding, D., 2013. Personal communication. Rio Tinto Technology & Innovation.

John, R.S., Batchelor, A.R., Ivanov, D., Udoudo, O.B., Jones, D.A., Dodds, C., Kingman, S.W., 2015. Understanding microwave induced sorting of porphyry copper ores. Minerals Engineering 84, 77-87.

Katrib, J., Dimitrakis, G., Batchelor, A.R., Dodds, C., Kingman, S.W., 2016. Design of a high throughput continuous microwave system. Computers and Chemical Engineering (Under Review).

Lessard, J., de Bakker, J., McHugh, L., 2014. Development of ore sorting and its impact on mineral processing economics. Minerals Engineering 65, 88-97.

Lessard, J., Sweetser, W., Bartram, K., Figueroa, J., McHugh, L., 2016. Bridging the gap: Understanding the economic impact of ore sorting on a mineral processing circuit. Minerals Engineering 91, 92-99.

Meredith, R.J., 1998. Engineers' handbook of industrial microwave processing. The Institution of Electrical Engineers, London, UK.

Napier-Munn, T., 2015. Is progress in energy-efficient comminution doomed? Minerals Engineering 73, 1-6.

Pokrajcic, Z., Morrison, R., Johnson, B., 2009. Designing for a reduced carbon footprint at Greenfield and operating comminution plants, Recent Advances in Mineral Processing Plant Design. Society for Mining, Metallurgy, and Exploration, pp. 560-570.

Powell, M., Bye, A., 2009. Beyond mine-to-mill: Circuit design for energy efficient resource utilisation, Tenth Mill Operators Conference 2009, Proceedings. AusIMM, pp. 357-364.

Sivamohan, R., Forssberg, E., 1991. Electronic sorting and other preconcentration methods. Minerals Engineering 4, 797-814.

Van Weert, G., Kondos, P., 2007. Infrared recognition of high sulphide and carbonaceous rocks after microwave heating, 39th Annual Meeting of the Canadian Mineral Processors, Ottowa, Ontario, Canada, pp. 345-363.

Van Weert, G., Kondos, P., Gluck, E., 2009. Upgrading molybdenite ores between mine and mill using microwave/infrared (MW/IR) sorting technology, 41st Annual Meeting of the Canadian Mineral Processors, Ottowa, Ontario, Canada.

http://dx.doi.org/10.1016/j.mineng.2016.07.009

Supplementary Information

Table S.1

Mass and copper distributions across copper grade classes

Sample ID	Mass Distribution (%)					Copper Distribution (%)				
	Barren	Marginal Grade	Low Grade	High Grade	Very High Grade	Barren	Marginal Grade	Low Grade	High Grade	Very High Grade
	<0.1%Cu	0.1-0.25%Cu	0.25-0.5%Cu	0.5-1%Cu	>1%Cu	<0.1%Cu	0.1-0.25%Cu	0.25-0.5%Cu	0.5-1%Cu	>1%Cu
-76.2+50.8mm Size Class										
9	14.8	45.3	18.1	18.7	3.1	3.1	25.1	19.8	40.9	11.1
9W	37.6	52.8	9.6	0.0	0.0	16.8	55.7	27.5	0.0	0.0
10	0.0	2.5	30.1	42.5	24.8	0.0	0.7	16.1	39.1	44.1
10W	35.2	38.3	18.5	8.0	0.0	6.9	28.5	38.3	26.3	0.0
11	24.9	46.5	22.1	6.6	0.0	6.4	35.2	36.2	22.2	0.0
11W	35.6	30.2	17.7	13.2	3.3	5.5	19.7	22.7	32.5	19.5
14	21.3	30.6	26.1	19.4	2.6	3.4	16.7	30.2	38.9	10.9
14W	13.5	22.8	39.3	21.8	2.6	2.0	10.9	40.1	38.7	8.3
15W	39.1	30.5	18.7	10.8	0.9	7.5	23.4	30.7	32.6	5.9
16W	56.7	28.9	9.4	4.3	0.8	12.5	33.5	25.0	21.8	7.2
17W	50.2	17.5	17.9	14.5	0.0	6.7	12.9	30.3	50.2	0.0
-50.8+25.4mm Size Class										
9	9.0	29.2	36.4	18.8	6.6	0.8	12.6	33.0	34.3	19.4
9W	41.2	48.9	9.9	0.0	0.0	14.6	61.8	23.5	0.0	0.0
10	0.0	2.1	43.0	35.1	19.8	0.0	0.6	23.3	34.8	41.2
10W	25.2	44.4	16.4	14.0	0.0	5.5	29.3	23.1	42.0	0.0
11	36.7	31.4	18.7	11.4	1.8	7.5	20.7	24.6	31.0	16.2
11W	37.5	30.5	22.1	4.9	5.0	5.6	19.6	30.1	11.9	32.9
14	30.9	19.8	25.2	16.2	8.0	3.6	8.8	24.2	27.7	35.8
14W	24.3	25.8	27.4	18.5	4.0	3.8	12.9	29.2	37.9	16.2
15W	51.7	16.5	17.3	8.0	6.5	7.3	10.4	24.4	21.9	36.0
16W	73.8	15.0	7.8	3.4	0.0	25.5	25.7	25.5	23.2	0.0
17W	56.5	18.3	13.3	10.2	1.6	8.0	16.8	28.0	36.5	10.6
-25.4+12.7mm Size Class										
9	15.7	14.7	28.4	22.2	18.9	1.2	4.1	18.5	25.8	50.3
9W	59.2	27.8	4.3	4.0	4.8	14.0	27.0	8.0	16.7	34.3
10	1.0	8.0	36.4	34.9	19.8	0.1	2.3	20.3	35.6	41.7
10W	38.9	39.8	9.2	7.8	4.4	6.6	24.6	10.5	20.4	37.9
11	45.8	10.7	18.9	14.2	10.3	5.0	5.2	17.7	29.3	42.8
11W	39.1	30.1	15.8	6.7	8.2	6.8	17.2	19.9	15.3	40.9
14	38.7	26.6	16.5	13.4	4.7	4.7	14.7	20.2	32.3	28.2
14W	26.1	29.4	20.3	16.9	7.2	3.1	14.5	21.1	33.4	28.0
15W	62.6	13.4	10.8	9.2	4.0	9.6	11.3	19.7	32.3	27.2
16W	77.6	15.4	5.4	0.0	1.6	22.6	32.3	22.1	0.0	23.1
17W	66.8	16.0	9.0	4.1	4.1	8.2	16.7	22.6	16.4	36.1

http://dx.doi.org/10.1016/j.mineng.2016.07.009

Table S.2

Laboratory test conditions summary

Sample ID	Pilot Plant Equivalent Test (#)	Belt Speed (m/s)	Belt Loading (kg/m)	Feed Rate (t/h)	Forward Power (kW)	Absorbed Power (kW)	Microwave Dose (kWh/t)	Head Grade (%Cu)	Feed Temp. 4σ (°C)
-76.2+50.8mm Size Class									
9	1-7	0.30	32.0	34.6	28.5-28.8	26.6	0.769-0.770	0.287	0.72-1.23
9W	1-6	0.50	31.1	56.0	44.0-46.1	39.0-41.0	0.696-0.732	0.140	1.08-3.75
10	1-3	0.40	36.2	52.1	42.1-47.7	39.3-42.3	0.754-0.810	0.753	0.50-0.69
10W	1-6	0.40	34.7	49.9	28.3-29.2	25.9	0.518-0.519	0.202	0.87-0.98
11	1-6	0.25-0.40	33.6	30.2-48.3	24.1-29.3	23.0-37.9	0.760-0.784	0.210	0.95-1.30
11W	1-6	0.30	40.3	43.5	23.5-23.6	22.7	0.521-0.523	0.259	1.20-1.41
14	1-6	0.40	28.3	40.7	41.8-42.0	40.7	0.999	0.311	1.37-1.59
14W	1-4	0.40-0.50	30.6	44.0-55.0	35.2-45.3	33.9-44.1	0.771-0.801	0.356	0.97-5.09
15W	1-5	0.40	26.9	38.7	40.9-41.6	39.1-39.4	1.009-1.017	0.219	1.33-1.50
16W	1-6	0.40	30.6	44.0	45.1-45.2	44.0-44.2	0.999-1.006	0.135	0.59-0.96
17W	1-15	0.40	27.7	39.9	42.0-42.2	38.9-39.3	0.974-0.984	0.219	1.25-1.79
-50.8+25.4mm Size Class									
9	1-8	0.40	22.5	32.4	35.8-36.4	32.9-34.1	1.015-1.053	0.415	0.61-0.73
9W	1-6	0.75	21.8	58.9	43.5-46.4	38.8-43.7	0.657-0.742	0.120	0.71-0.78
10	1-3	0.50	21.4	38.5	28.6-29.9	25.4-27.5	0.659-0.713	0.707	0.73-0.93
10W	1-7	0.50	19.0	34.2	22.6-23.0	18.0	0.525-0.527	0.255	0.85-0.94
11	1-6	0.30	26.9	29.1	23.5	21.2-21.5	0.730-0.741	0.265	0.55-0.78
11W	1-6	0.40	19.8	28.5	23.5-23.6	21.6-21.8	0.756-0.764	0.260	0.80-1.09
14	1-8	0.40	16.8	24.2	25.4-25.5	24.4-24.6	1.007-1.016	0.364	0.76-0.77
14W	1-4	0.50	14.6	26.3	28.2-28.6	26.7-27.2	1.014-1.033	0.354	0.66-0.68
15W	1-5	0.40	16.4	23.5	25.5-26.2	23.5-24.3	0.998-1.032	0.272	0.44-1.24
16W	1-4	0.50	16.9	30.5	31.5-31.6	30.4-30.6	0.998-1.005	0.093	0.31-0.66
17W	1-10	0.50	15.6	28.0	29.9	28.2-28.3	1.004-1.007	0.176	0.68-0.75
-25.4+12.7mm Size Class									
9	1-16	0.40	9.2	13.2	17.2	13.3-13.4	1.005-1.016	0.571	0.32-0.40
	17-22	0.60	9.2	19.8	19.0-19.3	15.0-15.2	0.758-0.766	0.571	0.33-0.37
9W	1-5	0.75	9.1	24.4	34.1-32.4	23.7-24.9	0.970-1.020	0.163	0.61-0.80
	6-9	0.75	9.1	24.4	20.7-21.9	17.7-18.5	0.724-0.756	0.163	0.50-0.59
10	1-3	0.50	11.6	20.8	26.3-33.1	24.6-25.4	1.181-1.206	0.656	0.46-0.63
10W	1-6	0.50	9.0	16.2	20.0-20.1	15.8-16.7	0.972-1.031	0.273	0.52-0.53
11	1-4	0.50	10.3	18.5	21.7	18.3-18.6	0.986-1.002	0.342	0.58-0.73
	5-13	0.50	10.3	18.5	17.3-17.6	13.6-14.2	0.734-0.767	0.342	0.59-0.83
11W	1-4	0.50	10.0	18.1	18.6-18.7	13.3-13.7	0.737-0.760	0.293	0.41-0.44
	5-8	0.50	10.0	18.1	13.9	9.5	0.525	0.293	0.43
14	1-4	0.60	9.6	20.7	17.0	15.0	0.725	0.289	0.39-0.41
	5-8	-	-	-	-	-	-	-	-
14W	1-4	0.60	8.5	18.4	16.0	14.2	0.770	0.341	0.41
	5-8	-	-	-	-	-	-	-	-
15W	1-4	0.60	9.0	19.4	21.6-23.2	19.4-20.0	0.995-1.029	0.202	0.48-0.88
	5-6	-	-	-	-	-	-	-	-
16W	1-6	0.60	7.8	16.9	14.0	12.9	0.764	0.082	0.61
17W	1-4	0.50	10.3	18.5	21.7	18.2-18.5	0.983-0.999	0.156	0.42-0.58
	5-7	0.50	10.3	18.5	17.6	14.2	0.767	0.156	0.59

http://dx.doi.org/10.1016/j.mineng.2016.07.009

Table S.3

Pilot plant test conditions summary

Sample ID	Test (#)	Belt Speed (m/s)	Belt Loading (kg/m)	Feed Rate (t/h)	Forward Power (kW)	Absorbed Power (kW)	Microwave Dose (kWh/t)	Head Grade (%Cu)	Feed Temp. 4σ (°C)
-76.2+50.8mm Size Class									
9	1-7	0.23-0.24	41.1-43.4	35.8-36.3	31.1-31.5	30.8-31.1	0.857-0.877	0.321-0.367	1.12-1.52
9W	1-6	0.23-0.26	37.1-43.0	34.6-36.0	23.4-24.5	20.4-23.5	0.661-0.684	0.146-0.192	0.61-1.44
10	1-3	0.46	21.3-21.5	35.6-35.9	26.7-26.8	25.8-26.1	0.744-0.750	0.692-0.735	0.84-1.25
10W	1-6	0.23-0.27	37.1-42.9	35.6-36.1	18.3-20.3	17.5-19.6	0.512-0.566	0.207-0.288	0.63-1.42
11	1-6	0.23-0.27	38.0-42.4	35.4-36.5	28.7-29.0	28.4-28.6	0.793-0.818	0.209-0.292	0.63-1.07
11W	1-6	0.23-0.25	39.8-43.1	35.4-36.3	25.7-25.9	25.5-25.7	0.718-0.732	0.254-0.301	1.08-1.26
14	1-6	0.28	34.6-36.5	34.9-36.6	38.1-38.3	37.8-38.0	1.041-1.103	0.259-0.345	0.59-1.05
14W	1-4	0.28	35.4-36.7	35.5-36.7	38.2-38.3	37.9	1.040-1.078	0.211-0.236	0.70-0.76
15W	1-5	0.28	35.3-35.8	35.3-35.9	38.1-38.2	37.9-38.0	1.062-1.081	0.205-0.242	0.80-1.04
16W	1-6	0.28	35.3-36.1	35.4-36.2	38.1-38.3	37.8-38.0	1.056-1.082	0.088-0.115	0.60-0.91
17W	1-15	0.23-0.28	30.3-42.9	30.3-36.2	31.8-43.9	31.4-43.6	1.048-1.233	0.140-0.217	0.52-1.13
-50.8+25.4mm Size Class									
9	1-8	0.24-0.27	35.3-41.9	34.8-36.1	31.4-31.7	29.1-31.3	0.872-0.910	0.383-0.512	0.79-1.14
9W	1-6	0.24-0.26	38.1-42.4	35.6-36.8	23.4-24.3	21.1-23.0	0.630-0.677	0.128-0.169	0.79-1.10
10	1-3	0.23-0.93	12.7-50.8	42.3-42.4	30.6-30.7	30.0	0.723-0.724	0.640-0.676	0.50-0.72
10W	1-7	0.23-0.32	30.9-42.9	34.8-36.1	18.2-21.4	16.9-20.8	0.506	0.612	0.175-0.250
11	1-6	0.23	42.6-43.2	35.6-36.1	29.7-29.8	29.3-29.4	0.825-0.838	0.263-0.342	0.50-0.78
11W	1-6	0.23-0.25	40.4-42.9	35.9-36.2	25.8	25.6-25.7	0.710-0.720	0.241-0.296	0.92-1.49
14	1-8	0.28	35.8	35.6-35.9	38.1-38.3	38.0-38.2	1.060-1.071	0.212-0.299	0.57-1.16
14W	1-4	0.28	35.2-35.9	35.3-36.0	38.2-38.3	38.2	1.062-1.084	0.161-0.217	0.43-0.53
15W	1-5	0.28	35.9-36.2	36.0-36.3	38.1-38.3	38.1-38.2	1.052-1.063	0.179-0.233	0.77-0.96
16W	1-4	0.28	35.1-36.0	35.1-36.0	38.2-38.3	38.2	1.061-1.089	0.087-0.108	0.58-0.67
17W	1-10	0.24-0.37	26.9-41.8	29.5-35.9	31.5-54.9	31.4-54.7	1.062-1.560	0.120-0.199	0.56-0.85
-25.4+12.7mm Size Class									
9	1-16	0.23-0.39	15.6-34.4	17.6-30.2	18.4-41.2	18.3-41.1	0.879-1.398	0.361-0.480	0.43-0.77
	17-22	0.28-0.58	8.5-26.7	17.2-27.3	13.3-19.0	13.2-19.0	0.678-0.775	0.441-0.473	0.59-0.84
9W	1-5	0.35	14.4-15.3	18.0-19.2	17.3-18.5	17.2-18.4	0.900-1.024	0.139-0.159	0.37-0.38
	6-9	0.26-0.27	26.8-27.5	25.7-26.5	20.6	20.5-20.6	0.779-0.799	0.151-0.156	0.34-0.39
10	1-3	0.23-0.25	33.1-36.2	28.9-30.2	30.4-30.6	30.1-30.3	1.007-1.051	0.584-0.598	0.38-0.45
10W	1-6	0.26-0.28	29.8-32.4	29.4-30.5	30.0-30.6	28.0-29.2	1.05-1.043	0.193-0.238	0.34-0.44
11	1-4	0.28	28.6-30.4	28.7-30.6	30.7-30.8	30.3-30.5	1.010-1.073	0.223-0.297	0.37-0.47
	5-13	0.35-0.58	8.2-21.2	17.0-26.5	11.5-18.5	11.5-18.4	0.657-0.712	0.252-0.270	0.38-1.18
11W	1-4	0.23	30.8-31.6	25.7-26.4	25.8	25.8	0.977-1.003	0.299-0.310	0.42-0.48
	5-8	0.46	10.7-10.8	17.8-18.0	10.2	10.1	0.567-0.573	0.300-0.353	0.42-0.56
14	1-4	0.26	27.7-28.3	25.5-26.0	20.6	20.5-20.6	0.792-0.809	0.245-0.263	0.33-0.36
	5-8	0.44-0.46	11.3-11.7	18.5-18.7	10.2	10.2	0.546-0.552	0.259-0.266	0.35-0.51
14W	1-4	0.23	21.3-21.6	17.8-18.1	14.3	14.3	0.794-0.805	0.212-0.231	0.38-0.58
	5-8	0.25-0.27	26.7-31.0	26.1-27.4	15.3-15.4	15.3-15.4	0.561-0.587	0.216-0.233	0.35-0.41
15W	1-4	0.28	25.3-26.5	25.4-26.5	25.8-25.9	25.7-25.8	0.976-1.017	0.182-0.194	0.38-0.44
	5-6	0.23	20.9-21.2	17.4-17.7	10.2	10.2	0.577-0.584	0.172-0.182	0.42-0.53
16W	1-6	0.23-0.25	20.2-32.0	17.6-26.7	14.3-21.7	14.3-21.7	0.797-0.841	0.097-0.121	0.42-0.60
17W	1-4	0.25-0.26	19.2-19.5	16.7-17.9	18.4-18.5	18.4	1.033-1.103	0.139-0.150	0.35-0.40
	5-7	0.26	27.8-29.3	26.3-28.0	20.6	20.5-20.6	0.736-0.784	0.147-0.152	0.32-0.53

http://dx.doi.org/10.1016/j.mineng.2016.07.009

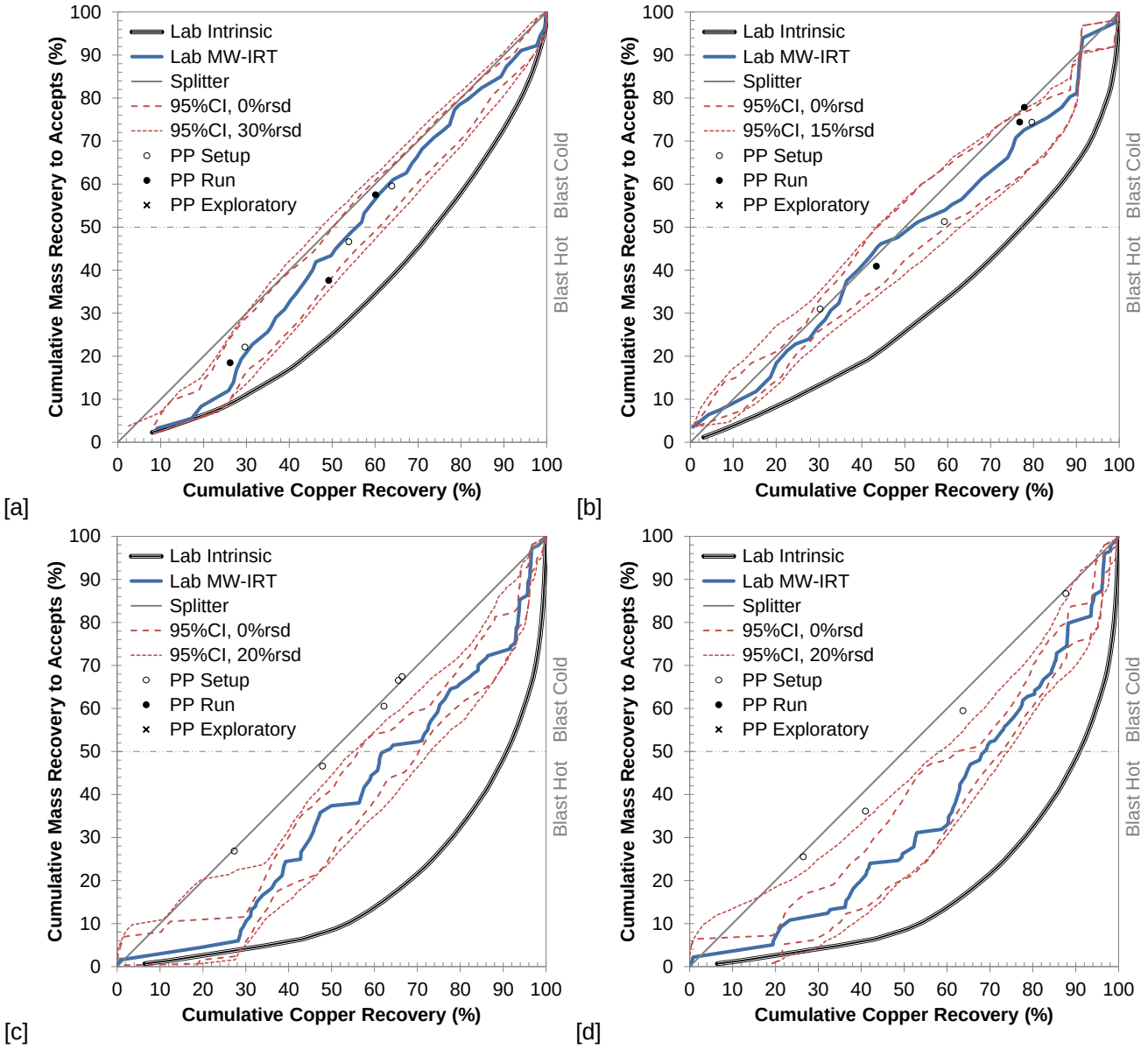

Figure S.1: Sample #9W sortability performance for [a] -76.2+50.8mm fragments at ~0.75kWh/t, [b] -50.8+25.4mm fragments at ~0.75kWh/t, [c] -25.4+12.7mm at ~1kWh/t, and [d] -25.4+12.7mm at ~0.75kWh/t

http://dx.doi.org/10.1016/j.mineng.2016.07.009

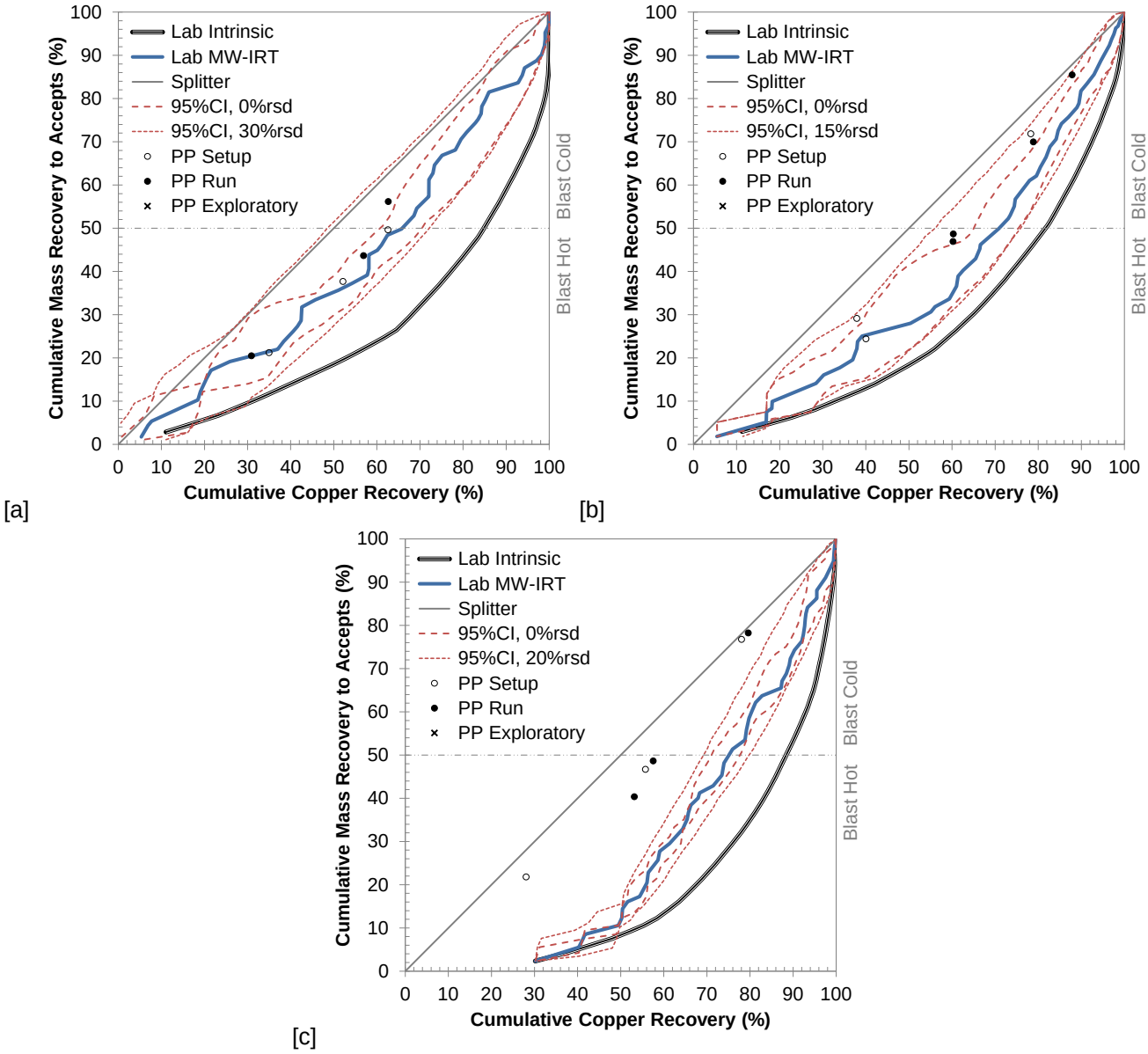

Figure S.2: Sample #10W sortability performance for [a] -76.2+50.8mm fragments at ~0.5kWh/t, [b] -50.8+25.4mm fragments at ~0.5kWh/t, and [c] -25.4+12.7mm at ~1kWh/t

http://dx.doi.org/10.1016/j.mineng.2016.07.009

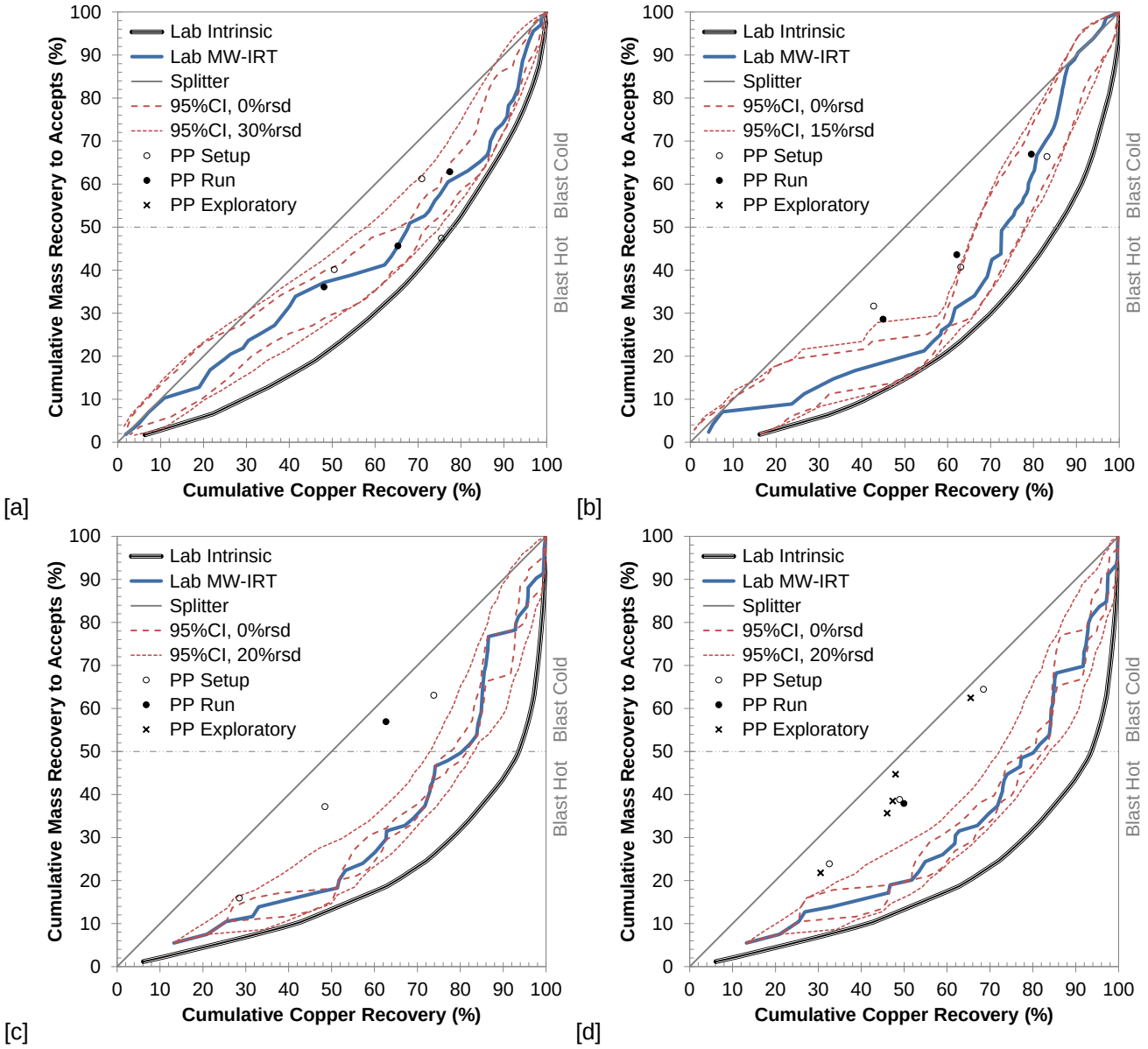

Figure S.3: Sample #11 sortability performance for [a] -76.2+50.8mm fragments at ~0.75kWh/t, [b] -50.8+25.4mm fragments at ~0.75kWh/t, [c] -25.4+12.7mm at ~1kWh/t, and [d] -25.4+12.7mm at ~0.75kWh/t

http://dx.doi.org/10.1016/j.mineng.2016.07.009

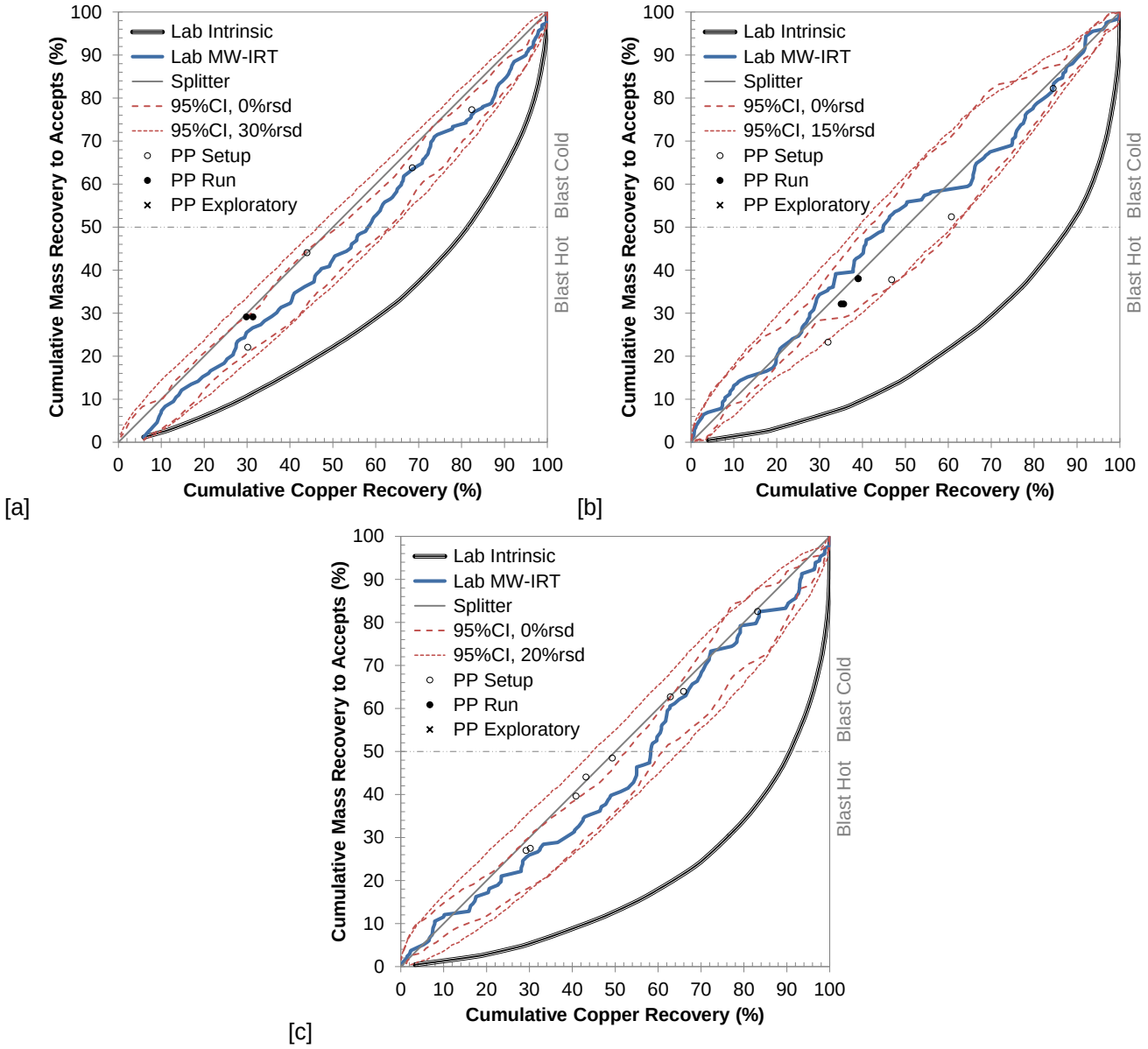

Figure S.4: Sample #14 sortability performance for [a] -76.2+50.8mm fragments at ~1kWh/t, [b] -50.8+25.4mm fragments at ~1kWh/t, and [c] -25.4+12.7mm at ~0.75kWh/t and ~0.5kWh/t

http://dx.doi.org/10.1016/j.mineng.2016.07.009

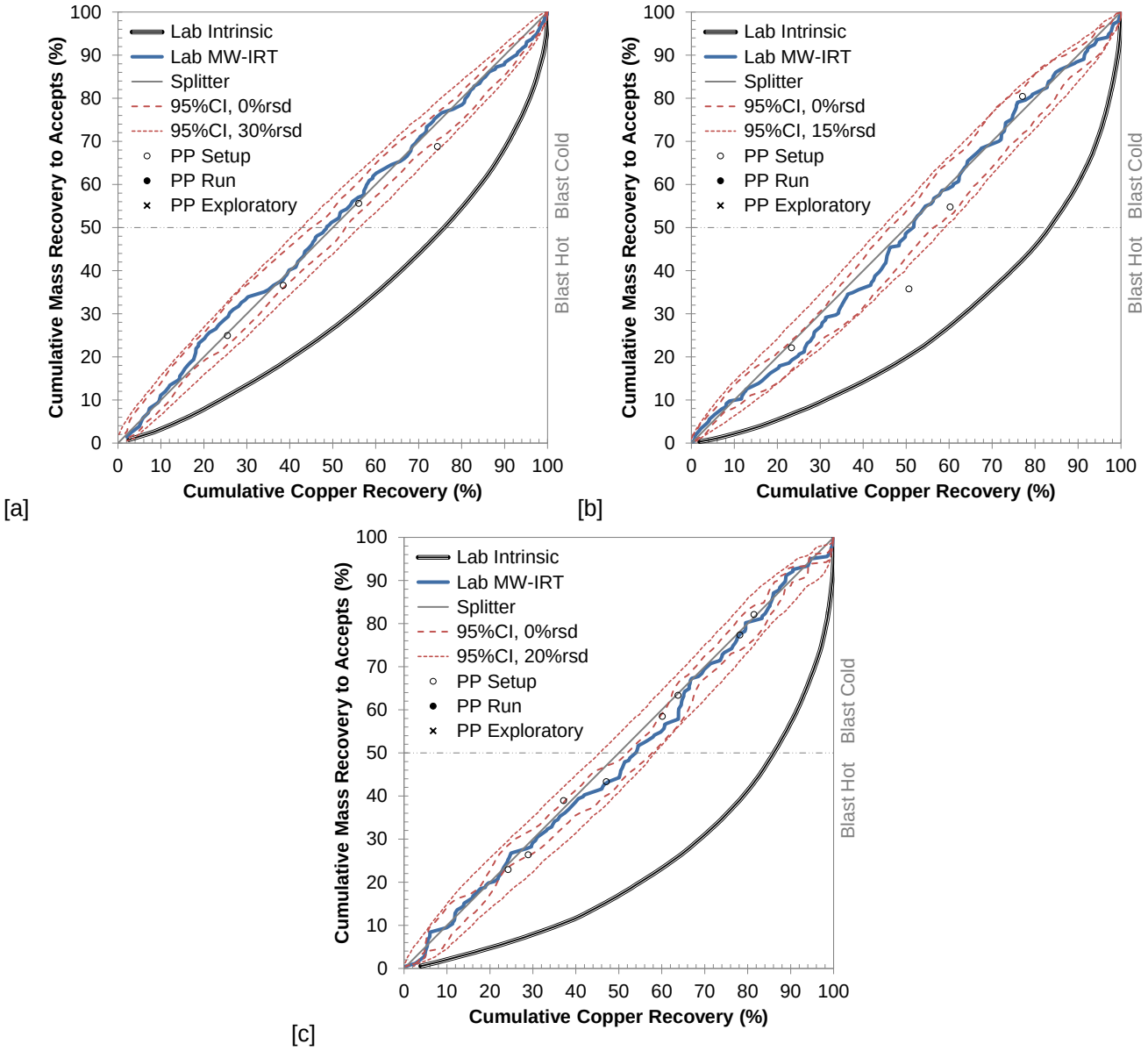

Figure S.5: Sample #14W sortability performance for [a] -76.2+50.8mm fragments at ~1kWh/t, [b] -50.8+25.4mm fragments at ~1kWh/t, and [c] -25.4+12.7mm at ~0.75kWh/t and ~0.5kWh/t

http://dx.doi.org/10.1016/j.mineng.2016.07.009

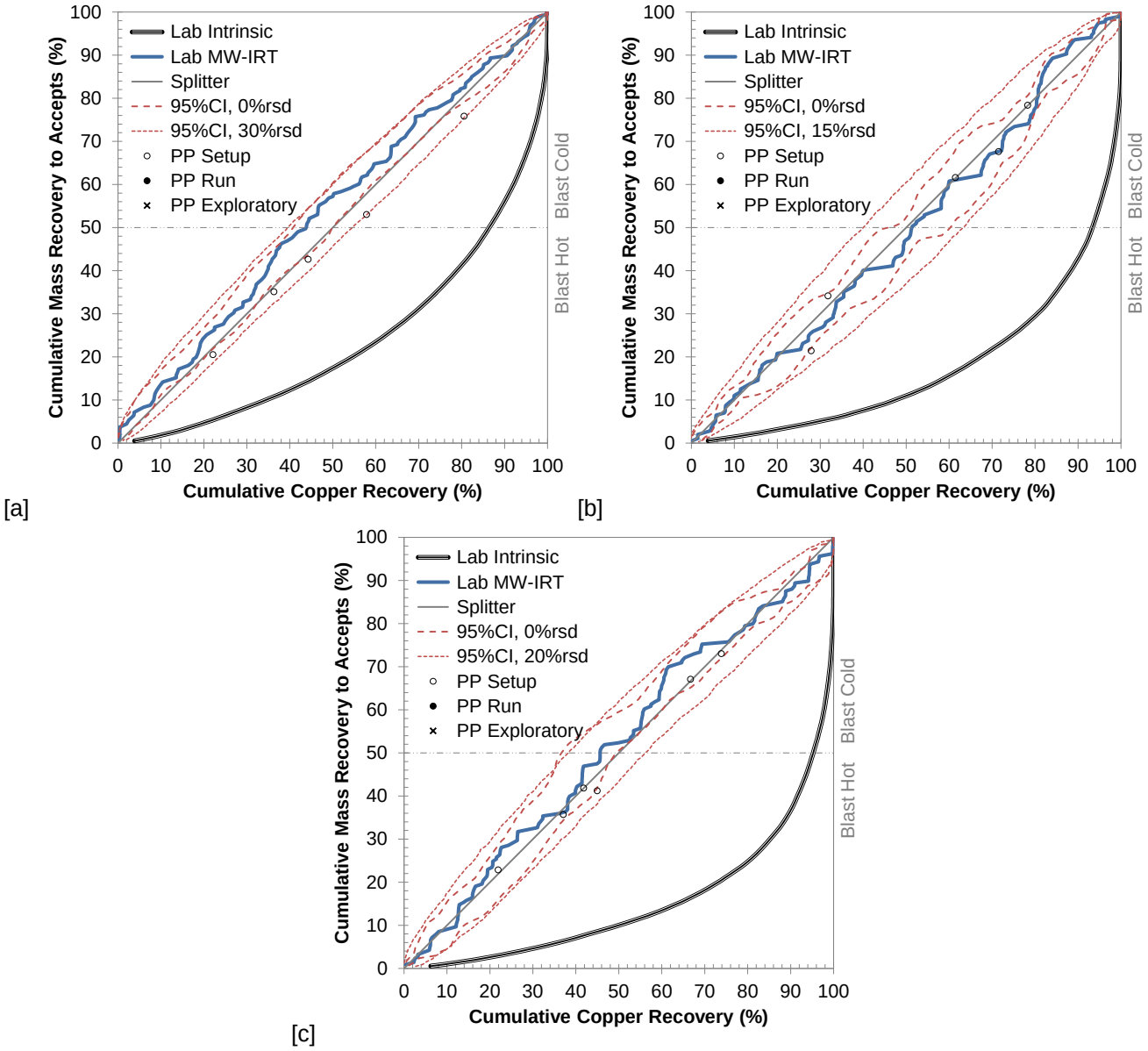

Figure S.6: Sample #15W sortability performance for [a] -76.2+50.8mm fragments at ~1kWh/t, [b] -50.8+25.4mm fragments at ~1kWh/t, and [c] -25.4+12.7mm at ~1kWh/t and ~0.5kWh/t

http://dx.doi.org/10.1016/j.mineng.2016.07.009

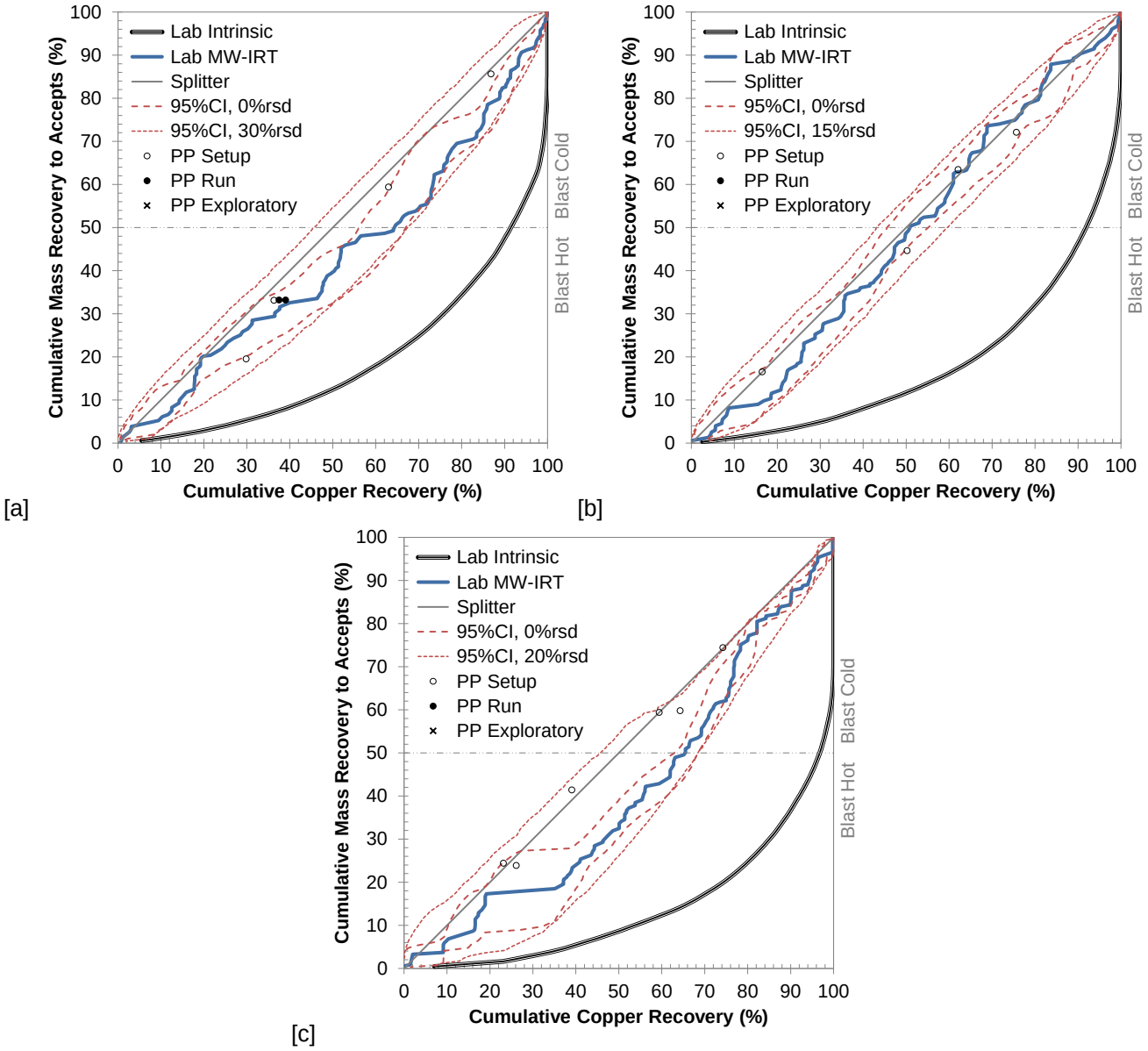

Figure S.7: Sample #16W sortability performance for [a] -76.2+50.8mm fragments at ~1kWh/t, [b] -50.8+25.4mm fragments at ~1kWh/t, and [c] -25.4+12.7mm at ~0.75kWh/t

http://dx.doi.org/10.1016/j.mineng.2016.07.009

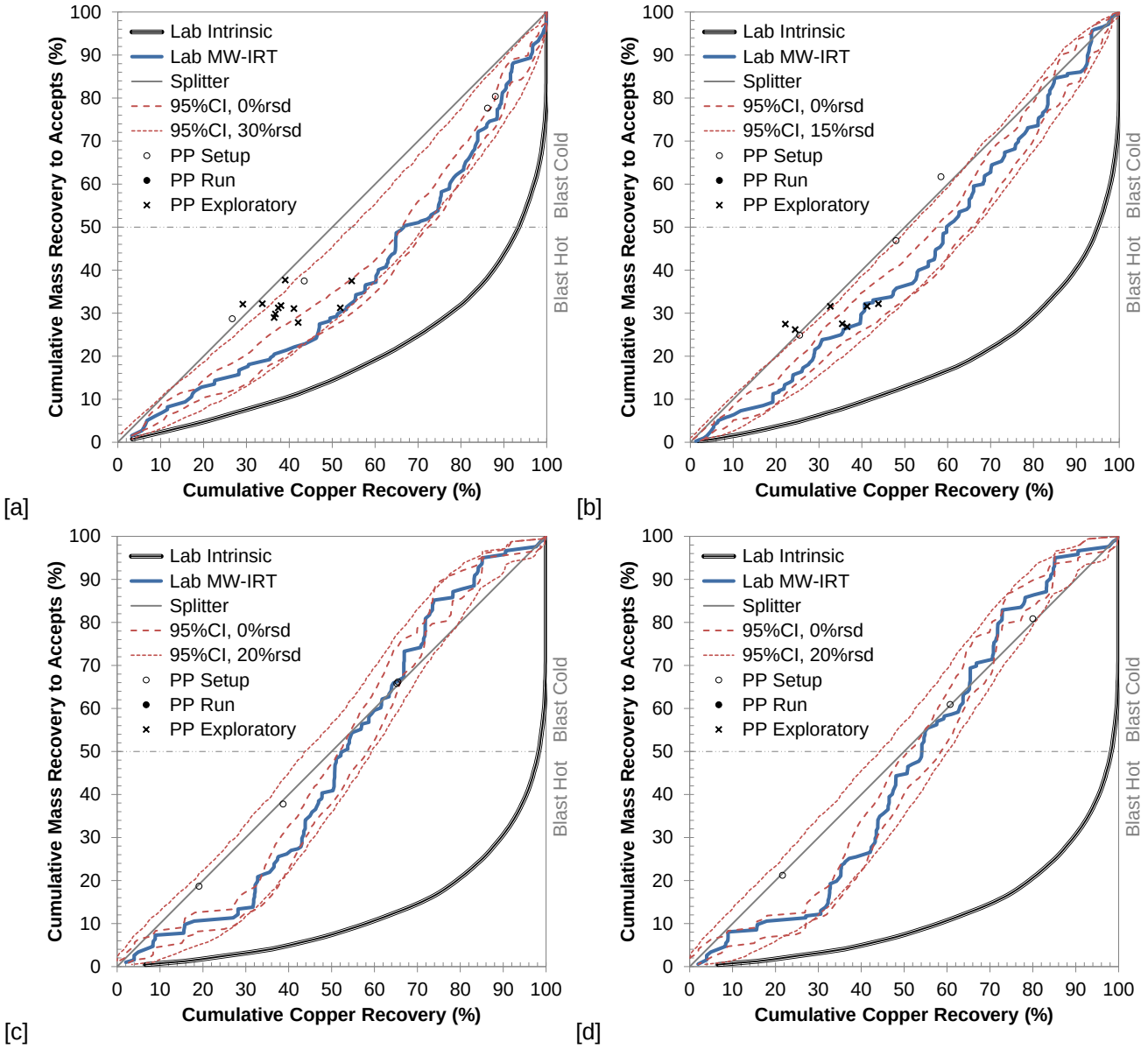

Figure S.8: Sample #17W sortability performance for [a] -76.2+50.8mm fragments at ~1kWh/t, [b] -50.8+25.4mm fragments at ~1kWh/t, [c] -25.4+12.7mm at ~1kWh/t, and [d] -25.4+12.7mm at ~0.75kWh/t

http://dx.doi.org/10.1016/j.mineng.2016.07.009